AD-A133 157 A MAXIMUM LIKELIHOOD PROGRAM FOR NON-LINEAR SYSTEM IDENTIFICATION WITH AP..(U) AERONAUTICAL RESEARCH LABS MELBOURNE (AUSTRALIA) R A FEIK JUL 82 1/1

UNCLASSIFIED ARL/AERO NOTE-411 F/G 12/1 NL

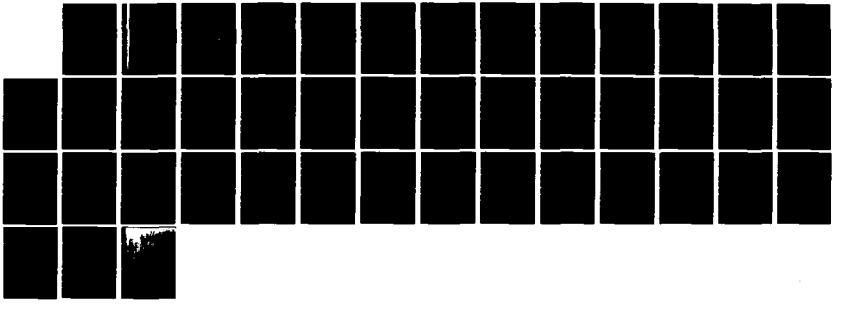

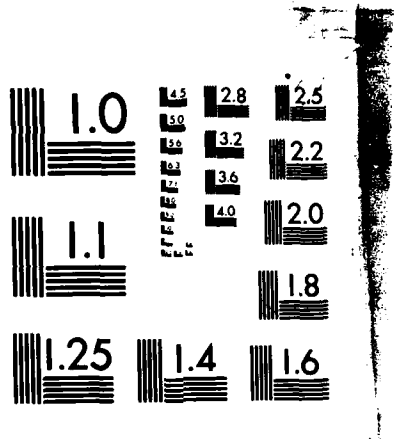

MICROCOPY RESOLUTION TEST CHART
NATIONAL BUREAU OF STANDARDS-1963-A

(12)

ARL-AERO-NOTE-411

AR-002-8[illegible]

DEPARTMENT OF DEFENCE SUPPORT

DEFENCE SCIENCE AND TECHNOLOGY ORGANISATION

AERONAUTICAL RESEARCH LABORATORIES

MELBOURNE, VICTORIA

AERODYNAMICS NOTE 411

A MAXIMUM LIKELIHOOD PROGRAM FOR NON-LINEAR SYSTEM IDENTIFICATION WITH APPLICATION TO AIRCRAFT FLIGHT DATA COMPATIBILITY CHECKING

by

R.A. FEIK

Approved for Public Release.

AR-002-896

DEPARTMENT OF DEFENCE SUPPORT
DEFENCE SCIENCE AND TECHNOLOGY ORGANISATION
AERONAUTICAL RESEARCH LABORATORIES

AERODYNAMICS NOTE 411

A MAXIMUM LIKELIHOOD PROGRAM FOR NON-LINEAR SYSTEM IDENTIFICATION WITH APPLICATION TO AIRCRAFT FLIGHT DATA COMPATIBILITY CHECKING

by

R.A. FEIK

SUMMARY

A Fortran program has been developed for the Maximum Likelihood Estimation of parameters in non-linear systems. The program structure uses subroutines to describe the problem and define problem-specific elements, while the main program is designed to be problem-independent as far as possible. In the present note an application of the program to compatibility checking of aircraft dynamic flight test data has been studied. Using simulated time histories of longitudinal manoeuvres, the conditions for satisfactory performance have been identified. It has been shown that for a practical manoeuvre shape, record length and sampling rate and for reasonable noise levels on the measured data, instrument errors can be identified to good accuracy and a set of compatible time histories reconstructed.

POSTAL ADDRESS: Director, Aeronautical Research Laboratories,
Box 4331, P.O., Melbourne, Victoria, 3001, Australia

CONTENTS

NOTATION

ax, ay, az	Linear accelerations in x, y, z directions, m/s^2
b_p, b_q, b_r, etc.	Offset bias in p, q, r, etc., measurements
g	Gravitational acceleration
h	Altitude, m
J	Cost functional to be minimised, equation (4)
L	Likelihood function, equation (3)
m	Length of observation vector $\mathbf{z}$
$\mathbf{n}$	measurement noise vector, equation (2)
n_q	Random noise in q measurement, equation (12)
N	Number of time points
p	Length of parameter vector, $\boldsymbol{\xi}$
p, q, r	Angular rates of roll, pitch and yaw, rad/s
$\mathbf{R}$	Measurement noise matrix
t	Time, sec
$\mathbf{u}$	Input vector
u, v, w	Velocities in x, y, z directions
V	Airspeed, m/s
$\mathbf{x}$	State vector
x, y, z	Reference body axes system
x_α, y_α, z_α	Body axes co-ordinates of angle-of-attack vane
x_β, y_β, z_β	Body axes co-ordinates of sideslip vane
$\mathbf{z}$	Observation vector
$\mathbf{z}_\xi$	Calculated output vector
α	Angle-of-attack, radians
β	Sideslip angle, radians
Δ	Increment
λ_p, λ_q, λ_r, etc.	Scale factor error in p, q, r, etc., measurements
ϕ, θ, ψ	Angle of roll, pitch and yaw, radians
$\boldsymbol{\xi}$	Parameter vector
∇_ξ	Gradient with respect to parameter vector, $\boldsymbol{\xi}$

	Subscripts
i	Time point index
j	Element of parameter vector, ξ_j
m	Measured value
out	Calculated output value
v	Sideslip or angle of attack vane
ξ_j	Partial derivative with respect to ξ_j element of parameter vector
	Superscript
T	Matrix or vector transpose

1. INTRODUCTION

The Aircraft Behaviour Studies—Fixed Wing Group has been actively involved in the determination of aircraft aerodynamic characteristics from flight test data for a number of years. Good results have been obtained (e.g. Ref. 1) when the mathematical model describing the aircraft motion is reasonably well known and linear or almost linear. In this case powerful methods are available (e.g. Ref. 2) which can identify the aerodynamic parameters in the presence of both state (or process) and measurement noise including instrumentation biases.

If the model is essentially non-linear then the problem becomes more difficult and is further complicated by the fact that such models are often not well defined. In particular this applies to the dynamics of aircraft at high incidence. Reference 3 provides a review of high angle of attack aerodynamics and points to the substantial effort in this area over recent years. Nevertheless the present state of knowledge is still largely descriptive. At the same time methods for identification of aerodynamics in high angle-of-attack regimes are in a relatively early stage of development and no standard approach has been established. Reference 4 is an example of one approach which makes clear the difficulty of the problem due to the presence of noise and instrument errors in the measurements, and uncertainties in the (non-linear) model structure. Because of this it would be desirable to separate out these two sources of error. This can conveniently be done in the aircraft case by separating the kinematics from the full dynamical description of the motion. The kinematic equations, relating accelerations, velocities and displacements are non-linear but well defined and, ideally, can be analysed to provide the unknown instrumentation biases and an optimal estimate of the state and measurement vectors. The resulting "error-free" records are then used in a full, but not necessarily well-defined, dynamic model. The methods of regression analysis, for example, can conveniently be applied in attempting to identify the parameters as well as the structure of this model. Regression analysis can be expected to give good results when measurement bias errors are absent (Ref. 8). This two-stage approach can, of course, be applied equally well to the linear well-defined model case as outlined in References 6, 7 and 8. In those references an Extended Kalman Filter is used in the first stage, i.e. for estimation of the aircraft dynamic state and of instrument systematic errors via the aircraft kinematic equations. Reference 6 obtains good results with a restricted number of variables while relying on high quality instrumentation. References 7 and 8 present a broader formulation but do not discuss the requirement for successful implementation such as noise levels and the need to specify them, record length, sampling rates, etc. Reference 9 points to some doubt on the suitability of an Extended Kalman Filter as a parameter estimator (for identifying systematic instrument errors), then proceeds to apply a maximum likelihood method, ignoring process noise, and presents some preliminary results. The neglect of process noise in the kinematic equations can be justified on the basis that it is small since instrumentation used for the measurement of the inputs is the most accurate available. Furthermore, modelling errors are absent since the kinematic equations can be considered to be exact. Reference 10 notes, for their restricted case and accurate instrumentation, that application of the Maximum Likelihood algorithm (no process noise) and the extended Kalman Filter/Smoother have been found to yield similar results.

In this note a Maximum Likelihood (ML) program is developed for application to a general non-linear system with no process noise. The user is required to specify the system under study via two subroutines, one setting out the differential equations of the system and the other specifying the system sensitivity matrix. Other problem-dependent subroutines are used for initialisation and for calculation of the output responses. The program has been applied here to the estimation of states and instrument systematic errors using the aircraft kinematic equations, as outlined above. The aim of this study is to assess the performance of the ML algorithm for this problem, to establish the conditions required for its successful implementation and to provide a baseline for comparison with other methods. To this end the effects of noise levels, record lengths and sampling rates, manoeuvre shape and the number of time histories matched, etc., have been studied and the results presented.

A theoretical description of the method including an outline of the ML program is presented in Section 2 and results of its application to the aircraft kinematic equations, using simulated data, are given in Section 3.

2. DESCRIPTION OF METHOD

A brief theoretical discussion of the Maximum Likelihood method is followed by a more detailed discussion of its application to the aircraft kinematic equations. Consideration of possible strong correlations among some of the parameters leads to several possible alternative approaches. A description of the computer program ends this section.

2.1 Theory

The system is assumed to be described by a set of non-linear dynamic equations of the form

$$\dot{\mathbf{x}}(t) = \mathbf{f}(\mathbf{x}(t),\mathbf{u}(t),\xi), \tag{1}$$

$$\mathbf{z}(t_i) = \mathbf{g}(\mathbf{x}(t_i),\mathbf{u}(t_i),\xi)+\mathbf{n}(t_i), \tag{2}$$

where $\mathbf{x}$ is the state vector,

$\mathbf{u}$ is the input vector,

$\mathbf{z}$ is the observation vector,

$\mathbf{n}$ is the measurement noise vector,

ξ is the vector of unknown parameters.

The state equation (1) is assumed to be free from process noise and the measurement noise is assumed to be zero mean white Gaussian noise. The measurements, $\mathbf{z}$, are made at a finite number of time points, t_i.

In order to estimate the unknown parameters a likelihood function, $L(\mathbf{z}|\xi)$, is defined which expresses the probability of obtaining the measurements, $\mathbf{z}$, given the parameters, ξ. The maximum likelihood (ML) estimate of ξ is the value which maximises $L(\mathbf{z}|\xi)$, evaluated with the measured responses. The ML estimate has a number of desirable properties, including consistency and efficiency (see Ref. 11). Using the Gaussian assumption for the measurement noise the likelihood function for the present case can be written (e.g. Ref. 11):

$$L(\mathbf{z}|\xi) = [2\pi^m|\mathbf{R}|\,]^{-N/2}\exp[-\tfrac{1}{2}\sum_{i=1}^{N}(\mathbf{z}(t_i)-\mathbf{z}_\xi(t_i))^T\mathbf{R}^{-1}(\mathbf{z}(t_i)-\mathbf{z}_\xi(t_i))] \tag{3}$$

where m is the length of the observation vector, $\mathbf{z}$,

N is the number of time points.

In equation (3) $\mathbf{z}_\zeta$ is calculated, for a particular ξ, from equations (1) and (2) neglecting the measurement noise, $\mathbf{n}$, while $\mathbf{R}$ is the covariance of the residuals, $\mathbf{z}(t_i)-\mathbf{z}_\zeta(t_i)$.

Taking the log of equation (3) for simplicity, the maximisation of L is equivalent to the minimisation of the cost functional

$$J(\xi,\mathbf{R}) = \tfrac{1}{2}mN\log 2\pi+\tfrac{1}{2}N\log|\mathbf{R}|+\tfrac{1}{2}\sum_{i=1}^{N}(\mathbf{z}(t_i)-\mathbf{z}_\xi(t_i))^T\mathbf{R}^{-1}(\mathbf{z}(t_i)-\mathbf{z}_\xi(t_i)) \tag{4}$$

For given $\mathbf{R}$ the first two terms of J are constant and the following simple cost functional results:

$$J(\xi) = \tfrac{1}{2}\sum_{i=1}^{N}(\mathbf{z}(t_i)-\mathbf{z}_\xi(t_i))^T\mathbf{R}^{-1}(\mathbf{z}(t_i)-\mathbf{z}_\xi(t_i)) \tag{5}$$

an estimate for $\mathbf{R}$ can be obtained by minimising $J(\xi,\mathbf{R})$ (eqn (4)) with respect to $\mathbf{R}$. This results in

$$\mathbf{R} = \frac{1}{N}\sum_{i=1}^{N}(\mathbf{z}(t_i)-\mathbf{z}_\xi(t_i))(\mathbf{z}(t_i)-\mathbf{z}_\xi(t_i))^T. \tag{6}$$

Thus the problem splits into two parts. For fixed ξ equation (6) maximises the likelihood function with respect to $\mathbf{R}$, while for given $\mathbf{R}$ the cost functional given by equation (5) is mini-

mised to estimate ξ. The optimisation algorithm used to achieve this is the modified Newton–Raphson algorithm as documented in Reference 12. Starting from an initial estimate for ξ, revised estimates are obtained iteratively from

$$\xi_{i+1} = \xi_i - [\nabla_\xi^2 J(\xi_i)]^{-1} [\nabla_\xi J(\xi_i)]^T. \tag{7}$$

The first gradient matrix is obtained directly from equation (5):

$$\nabla_\xi J(\xi) = \sum_{i=1}^{N} (\mathbf{z}(t_i) - \mathbf{z}_\xi(t_i))^T \mathbf{R}^{-1} [\nabla_\xi (\mathbf{z}_\xi(t_i))] \tag{8}$$

and an approximation to the second gradient is given by

$$\nabla_\xi^2 J(\xi) = \sum_{i=1}^{N} [\nabla_\xi (\mathbf{z}_\xi(t_i))]^T \mathbf{R}^{-1} \nabla_\xi (\mathbf{z}_\xi(t_i)). \tag{9}$$

The term $\nabla_\xi(\mathbf{z}_\xi(t_i))$ required to evaluate equations (8) and (9) is the sensitivity matrix to be obtained from the system equations.

Thus the iterative procedure used can be summarised as follows:

(1) start with initial values for ξ, $\mathbf{R}$;

(2) with fixed $\mathbf{R}$ use equations (7)–(9) to estimate a new ξ;

(3) from equation (6) obtain a new estimate of $\mathbf{R}$ using the revised ξ;

(4) repeat steps 2 and 3 until convergence.

In practice a few iterations are done with $\mathbf{R}$ fixed before step 3 is included, since the residual power can often be quite large in the first iteration or two and hence lead to a worse estimate of $\mathbf{R}$ than the starting value.

For the Gaussian case Reference 11 shows that the maximum likelihood estimator is asymptotically consistent and efficient, i.e. for large N the estimates for ξ are normally distributed about the true value with covariance given by the Cramer–Rao lower bound. Thus a measure of the accuracy of the estimates is given by (Ref 11):

$$\text{covariance}(\xi) = \left[\sum_{i=1}^{N} [\nabla_\xi (\mathbf{z}_\xi(t_i))]^T \mathbf{R}^{-1} \nabla_\xi (\mathbf{z}_\xi(t_i)) \right]^{-1} \tag{10}$$

The right-hand side of equation (10) can be seen to be the inverse of the second gradient matrix as approximated by equation (9).

2.2 Aircraft Kinematic Equations

The kinematic equations are a set of non-linear equations relating the position, velocity and acceleration of an aircraft with reference to a set of flat earth axes. The system can be defined as follows:

(i) *State vector*, $\mathbf{x} = [u,v,w,\phi,\theta,\psi,h]^T$

The state equations written in body axes (x,y,z) fixed in the aircraft with origin at the centre of gravity can be considered to be exact (e.g. Ref. 13):

$$\left.\begin{aligned}
\dot{u} &= -qw + rv + ax - g \sin\theta \\
\dot{v} &= -ru + pw + ay + g \cos\theta \sin\phi \\
\dot{w} &= qu - pv + az + g \cos\theta \cos\phi \\
\dot{\phi} &= p + q \sin\phi \tan\theta + r \cos\phi \tan\theta \\
\dot{\theta} &= q \cos\phi - r \sin\phi \\
\dot{\psi} &= q \sin\phi / \cos\theta + r \cos\phi / \cos\theta \\
\dot{h} &= u \sin\theta - v \cos\theta \sin\phi - w \cos\theta \cos\phi
\end{aligned}\right\} \tag{11}$$

where u, v, w are linear velocities in x, y, z directions,

ϕ, θ, ψ are roll, pitch and yaw attitudes

h is altitude,

p, q, r are roll, pitch and yaw angular rates,

ax, ay, az are linear acceleration in x, y, z directions,

g is gravitational constant.

Note that the $\dot{h}$ and $\dot{\psi}$ equations are not coupled into the other equations.

(ii) *Input vector*, $\mathbf{u} = [ax,ay,az,p,q,r]^T$

In general measured values for the input vector are corrupted by scale errors, instrument bias errors and random noise. For example, taking the pitch rate, q, we write

$$q = (1+\lambda_q)q_m+b_q+n_q, \tag{12}$$

where q_m is measured pitch rate,

λ_q represents scale factor error,

b_q represents instrument bias error,

n_q represents random noise,

with similar relations for the other elements of the input vector. If equation (12) and its counterparts are substituted into equation (11) then the unknown parameters λ_q, b_q, etc., appear explicitly in the state equation and in addition the random noise, n_q, gives rise to state, or process, noise. However accelerometers and gyros used in measuring the input quantities are the most accurate instruments used and random noise levels are generally small. Thus it is reasonable to assume that the process noise is negligible.

(iii) *Output vector*, $\mathbf{z} = [V,\beta_v,\alpha_v,\phi,\theta,\psi,h]^T$

Measurements of the output vector are corrupted by scale factor errors, biases and random noise. The equations for calculating the outputs are taken as:

$$\left.\begin{aligned}
V_{out} &= (1+\lambda_v)(u^2+v^2+w^2)^{1/2}+b_v \\
\beta_{v_{out}} &= (1+\lambda_\beta)\tan^{-1}\left[\frac{v}{u}+\frac{(rx_\beta-pz_\beta)}{u}\right]+b_\beta \\
\alpha_{v_{out}} &= (1+\lambda_\alpha)\tan^{-1}\left[\frac{w}{u}-\frac{(qx_\alpha-py_\alpha)}{u}\right]+b_\alpha \\
\phi_{out} &= (1+\lambda_\phi)\phi+b_\phi \\
\theta_{out} &= (1+\lambda_\theta)\theta+b_\theta \\
\psi_{out} &= (1+\lambda_\psi)\psi+b_\psi \\
h_{out} &= (1+\lambda_h)h+b_h
\end{aligned}\right\} \tag{13}$$

where V is airspeed,

α_v, β_v are incidence and sideslip angles at the sensor (vane).

The term $(rx_\beta-pz_\beta)/u$ in the β_v equation and the equivalent term in the α_v equation are corrections due to known sensor offsets $(x_\beta,y_\beta,z_\beta)$ and $(x_\alpha,y_\alpha,z_\alpha)$ relative to the centre of gravity.

Given the measurements of inputs and outputs the requirement is to estimate the biases and scale factors introduced in equations (12) and (13). In addition, although the state equation is noise free, the initial conditions are not known exactly and hence become part of the unknown parameter vector:

$$\begin{aligned}
\xi = [&b_{ax}, b_{ay}, b_{az}, b_p, b_q, b_r, b_v, b_\beta, b_\alpha, b_\phi, b_\theta, \\
&\lambda_{ax}, \lambda_{ay}, \lambda_{az}, \lambda_p, \lambda_q, \lambda_r, \lambda_v, \lambda_\beta, \lambda_\alpha, \lambda_\phi, \lambda_\theta, \lambda_\psi, \lambda_h, \\
&u(0), v(0), w(0), \phi(0), \theta(0)]^T.
\end{aligned} \tag{14}$$

The initial values and biases for yaw attitude, $\psi(0)$, b_ψ, and height $h(0)$, b_h can be assumed to be zero since there is no absolute reference implied in equation (11). The number of parameters in equation (14) can be reduced if some of the biases or scale factor errors can be assumed to be zero. For example, References 7 and 8 neglect all scale factor errors except for λ_v, λ_β, λ_α while Reference 9 retains only the bias errors.

For the present study, the problem has been scaled down further by considering the subset for longitudinal motions only and neglecting all scale factor errors. The reduced system can be summarised as follows:

(i) *State vector*, $\mathbf{x} = [u, w, \theta, h]^T$

$$\left.\begin{aligned} \dot{u} &= -(q_m+b_q)w+(ax_m+b_{ax})-g\sin\theta \\ \dot{w} &= (q_m+b_q)u+(az_m+b_{az})+g\cos\theta \\ \dot{\theta} &= q_m+b_q \\ \dot{h} &= u\sin\theta-w\cos\theta \end{aligned}\right\} \tag{14}$$

where $[ax_m, az_m, q_m]^T$ is the measured input vector.

(ii) *Output vector*, $\mathbf{z}_\xi = [V_{out}, \alpha_{v_{out}}, \theta_{out}, h_{out}]^T$

$$\left.\begin{aligned} V_{out} &= (u^2+w^2)^{1/2}+b_v \\ \alpha_{v_{out}} &= \tan^{-1}\left[\frac{w}{u}-\frac{(q_m+b_q)x_\alpha}{u}\right]+b_\alpha \\ \theta_{out} &= \theta+b_\theta \\ h_{out} &= h+b_h \end{aligned}\right\} \tag{15}$$

The unknown parameter vector to be estimated is now

$$\xi = [b_{ax}, b_{az}, b_q, b_v, b_\alpha, b_\theta, u(0), w(0), \theta(0)]^T. \tag{16}$$

The initial height, $h(0)$ and the bias b_h can be assumed to be zero and hence are not included in the parameter vector.

2.3 Sensitivity Matrix

The parameter estimation procedure as outlined in Section 2.1 requires the calculation of the sensitivity matrix, $\nabla_\xi(\mathbf{z}_\xi(t_i))$. For a measurement vector of dimension m and parameter vector of dimension p the sensitivity matrix is of order m by p with the (i, j) element being the partial derivative of the ith component of $\mathbf{z}_\xi$ with respect to the jth component of ξ. For example the (1, 2) element would be the partial derivative of V_{out} with respect to b_{az}, $V_{out,b_{az}}$. From equation (15) it follows that

$$V_{out,b_{az}} = (u\,.\,u_{b_{az}}+w\,.\,w_{b_{az}})/(u^2+w^2)^{1/2} \tag{17}$$

where u, w and the partial derivatives $u_{b_{az}}$ and $w_{b_{az}}$ are all functions of time. The velocity components u and w are obtained directly from the integration of equation (14). At the same time equations for $u_{b_{az}}$ and $w_{b_{az}}$ can readily be derived from the state equation (14). Thus, taking partial derivatives of equation (14) with respect to b_{az} provides the required set (note that $\theta_{b_{az}} = 0$):

$$\left.\begin{aligned} \dot{u}_{b_{az}} &= -(q_m+b_q)w_{b_{az}} \\ \dot{w}_{b_{az}} &= (q_m+b_q)u_{b_{az}}+1 \end{aligned}\right\} \tag{18}$$

with zero initial conditions. These equations (18) have to be integrated simultaneously with equations (14) to enable $V_{out,b_{az}}$ to be evaluated as a function of time from equation (17).

The complete sensitivity matrix for the present system is summarised in Appendix 1 and the full system of differential equations requiring to be integrated in order to calculate the elements of the sensitivity matrix is presented in Appendix 2.

It is a straightforward process to extend the system to include additional parameters if desired. Alternatively, if change of altitude is not measured it would be desirable to remove h from the sytem being considered. Thus the state vector and output vectors would reduce to dimension three. The sensitivity matrix would reduce from 4×9 to 3×9 and the total number of equations to be integrated would reduce from the 23 in Appendix 2 to 16.

2.4 Correlated Parameters

Examination of the output equations (15) reveals relationships between the unknown initial conditions $u(0)$, $w(0)$ and $\theta(0)$ and the unknown biases b_v, b_α and b_θ:

$$V_{out}(0) = (u^2(0)+w^2(0))^{\cdot\,2}+b_v \tag{19}$$

$$\alpha_{v_{out}}(0) = \tan^{-1}\left[\frac{w(0)}{u(0)} - \frac{(q_m(0)+b_q)\,.\,x_\alpha}{u(0)}\right]+b_\alpha \tag{20}$$

$$\theta_{out}(0) = \theta(0)+b_\theta. \tag{21}$$

For initially steady level flight ($q(0) = q_m(0)+b_q = 0$) equation (20) is slightly simplified and in addition a relation between $\theta(0)$, b_{ax} and b_{az} follows from equations (14):

$$\tan\theta(0) = -\left[\frac{ax_m(0) + b_{ax}}{az_m(0) + b_{az}}\right]. \tag{22}$$

In the absence of measurement noise it is required that calculated outputs are equal to measured outputs:

$$\left.\begin{aligned} V_{out}(0) &= V_m(0)\\ \alpha_{v_{out}}(0) &= \alpha_{v_m}(0)\\ \theta_{out} &= \theta_m(0)\end{aligned}\right\} \tag{23}$$

Thus any change in initial conditions must be accompanied by a change in one or more of the biases, e.g.,

$$\Delta b_\theta = -\Delta\theta(0), \text{ etc.} \tag{24}$$

This suggests that if the initial conditions are estimated then the related biases can be calculated directly without estimating them as independent parameters. The number of parameters to be estimated is thus reduced. However, at the same time, to be consistent, appropriate elements of the sensitivity matrix have to be modified. For example equation (24) implies that b_θ is now a function of $\theta(0)$ rather than an independent parameter and the partial derivative of b_θ with respect to $\theta(0)$ is -1. Using this with equation (21) gives the result for the sensitivity element $\theta_{out,\theta(0)} = 0$ rather than the previous value of 1. Similar modifications to the sensitivity matrix result when b_v and b_α are taken as functions of the initial conditions as implied by equations (19) and (20). Alternatively it is possible to consider $u(0)$, $w(0)$ and $\theta(0)$ to be functions of b_v, b_α and b_θ rather than the opposite, thus removing the initial conditions from the parameter vector in favour of b_v, b_z and b_θ. Finally, for initially steady level flight equation (22) suggests the possibility of calculating b_{ax} (or b_{az}) as a function of $\theta(0)$ and b_{az} (or b_{ax}). Modifications to the sensitivity matrix implied by these options are summarised in Appendix 3.

If, in the noise free case, all the parameters are estimated as though fully independent, the correlations between initial conditions and biases as expressed in equations (19) to (22) may well be expected to lead to less accurate or biased results. On the other hand, in the presence of measurement noise the relations given in equation (23) do not hold precisely so that the procedure outlined above may not be justified. The effect of noise will be examined further in Section 3.

2.5 Computer Program

The basic structure of the program is shown in Figure 1. In the first stage the input data provide all the information necessary to broadly define the problem. Thus, for example, the number of equations to be integrated and the parameters to be estimated are specified as well as the *a priori*, or initial, values for the parameters and for the weighting matrix **R**. In addition, fixed data, e.g. incidence vane location (x_α, y_α, z_α), etc., and data relating to computational aspects

such as step size, total number of time points and maximum number of iterations to be performed are provided at this stage. Finally, time histories of all the measured inputs, $\mathbf{u}(t_i)$, and outputs, $\mathbf{z}(t_i)$, are read in and stored in arrays, since they will be repeatedly called upon during the iteration process.

The iteration loop is commenced by setting up the arrays and matrices to be used in the subsequent calculation. For example, arrays representing the state variables and their derivatives with respect to time are initialised, together with the sensitivity matrix and the first gradient array and second gradient matrix (equations (8), (9)). The array and matrix formats used follow that given in Reference 12 thus enabling many of the utility subroutines provided there to be used in the current program. Much of the matrix manipulation in this block and in the block labelled "Estimate New Parameters" closely follows that documented in Reference 12. For the present study, in order to allow for flexibility in changing the number of parameters to be estimated, and hence the number of variables to be integrated (Appendix 2), the subroutine INIT has been written. Given the parameters to be estimated, INIT works out which equations need to be integrated and sets the initial conditions. Finally, before entering the time loop, the integrator is initialised, step size and required accuracy set, etc.

The time loop proceeds to integrate the necessary equations (Appendix 2) and concurrently evaluates the sensitivities (Appendix 1) and hence the gradients (equations (8), (9)) as well as the outputs (equation (15)), all based on the current parameter values. Integration is performed via the fourth order Runge–Kutta routine (subroutine ANINT) although a predictor–corrector method has also been used. The integration routine calls for derivative values which are supplied by subroutine DERIVS. When integration to the next time point is complete, sensitivities and outputs are evaluated via subroutines SENS and RESP respectively before the gradients can be calculated. The time loop proceeds step by step until the specified number of points is achieved. Note that on the first iteration, measured values of the states (or values deduced from the measurements) are used in calculating the gradient. This technique is useful if initial parameter values are far from the correct values (see Ref. 12).

All the information required for the estimation and updating of the parameters is now available (equation (7)) and this is now done. At the same time an updated weighting matrix is calculated using equation (6). As explained in Section 2.1 this step is only carried out after the first few iterations. The iteration loop proceeds until the specified number of iterations is complete. Alternatively, it would be possible to set a convergence criterion on the residuals but this has not been done here.

Finally, the correlation matrix, whose diagonal elements are the Cramer–Rao bounds, are calculated using equation (10). The output results include an iteration history comprising fit error (residuals), gradient, determinant of second gradient matrix and new values of estimated parameters after each iteration. The final values of the parameters and their Cramer–Rao bounds are then summarised followed by the normalised correlation matrix. A second output file contains time histories of the inputs and the measured and calculated outputs to be used for producing time history plots if required.

Since non-linear systems can vary greatly in their structure it is difficult to write a general program to cater for all possible variations. In the present case, although the main interest has been in the aircraft longitudinal kinematic equations, an attempt has been made to separate the problem-specific elements from the more generally applicable program elements. Thus the subroutines INIT, DERIVS, SENS and RESP are problem-specific and would have to be altered for each different system. Some alteration in the problem definition box (Fig. 1) would probably also be necessary. Such modifications are relatively simple and make it possible to apply the program to estimation of parameters in other non-linear systems of interest. For example, it could be used for estimating the aerodynamic parameters in a non-linear dynamic model of the aircraft using the "error-free" responses produced by the present program. However, for that particular problem, regression analysis would probably be more convenient to apply.

3. RESULTS AND DISCUSSION

The longitudinal system defined in equations (14)–(16) have been studied in some detail using simulated data. Measurement time histories were produced by an auxiliary program which allowed specified biases and noise levels to be set. Process as well as measurement noise could be specified in order to study the effect that process noise had on the results.

The study proceeds systematically by first looking at the no noise case and assessing the effects of changing the number of measured time histories to be matched and the performance of the different procedures (Section 2.4) designed to cope with correlated parameters. This is followed by results with measurement noise and then process noise added. The noise is in all cases white and Gaussian. The effects of record length, sampling rate and noise levels are investigated and finally the influence which manoeuvre shape has on the results is briefly examined. Some care has been taken to ensure that integration errors, due to too large an integration step size, are avoided while maintaining step size as large as possible in order to minimise computation time. Although a fourth order Runge–Kutta integration is normally used, a variable order and step size predictor–corrector method (Ref. 14) was also used, when checking integration accuracy.

3.1 Effect of Number of Responses Matched—No Noise

In order to assess the relative importance of each of the measured time histories, various combinations of two and three elements as well as the full four elements of the output vector (equation (15)) were matched. In the absence of measurement noise the weightings given to the records (i.e. the diagonal elements of **R**) were fixed approximately inversely proportional to the square of a typical expected noise level. The results are in fact fairly insensitive to variations in relative weightings.

In order to avoid the correlation problem discussed in Section 2.4 the biases b_v, b_x and b_θ were fixed at their correct values thus giving a six-element parameter vector (equation (16)). The manoeuvre shape used (Manoeuvre 1) is produced by the inputs shown in Figure 2. Starting from steady level flight the manoeuvre assumes a linear variation of longitudinal acceleration, ax, and periodic variations of normal acceleration, az, and pitch rate, q. The output airspeed, incidence and pitch attitude over a 60-second time span are shown in Figure 3, although only the first 20 seconds, at a sampling rate of 10 per second, was used at this stage. Figure 3 shows both the "measured" records and those calculated assuming zero biases but with initial values matched.

A summary of results, each obtained after four iterations and a typical processing time of 60 seconds on the PDP10 computer, is presented in Table 1. An indication of the relative accuracy of the estimates is provided by the number in parentheses which are the "Cramer–Rao" bounds computed with the fixed **R** matrix. It is clear from the results that the use of three matched time histories can produce almost as good results as four matched records. This is particularly true with the V, α, θ records which produce results for the estimated parameters, their confidence bounds and time history match errors (expressed as RMS error) in close agreement with the full match case. The use of only two time histories leads to a general deterioration of results with the V, α and V, θ cases being the least unacceptable.

It is concluded from this study that matching the height, h, record only provides a marginal improvement of the results compared to a V, α, θ match. Considering also the difficulties of obtaining accurate height measurements and the favourable reduction in the system equations when h is neglected (Section 2.3), height has been removed from the system equations in the following sections.

3.2 Effect of Parameter Correlations—No Noise

In this section all nine unknown parameters are estimated (equation (16)) with measurements assumed to be noise free. Because of the relations between the initial conditions and several

TABLE 1

Effect of Number of Time Histories Matched—No Noise

		Full match	Three time histories matched				Two time histories matched					
	Case No.	1	2	3	4	5	6	7	8	9	10	11
Parameter	True value	V, θ, α, h	V, α, θ	V, α, h	V, θ, h	α, θ, h	V, α	V, θ	V, h	α, θ	α, h	θ, h
b_{ax}, m/s^2	0·1	0·100	0·100	0·100	0·100	0·074	0·102	0·100	0·162	0·050	0·050	0·205
		(0·0123)	(0·0124)	(0·0125)	(0·0125)	(0·1158)	(0·1079)	(0·0209)	(0·0746)	(0·1573)	(0·1628)	(1·7887)
b_{az}, m/s^2	0·1	0·100	0·099	0·099	0·100	0·099	0·089	0·116	0·134	0·098	0·101	0·097
		(0·0047)	(0·0053)	(0·0096)	(0·0101)	(0·0053)	(0·0309)	(0·4294)	(0·0407)	(0·0077)	(0·0110)	(0·0550)
b_q, rad/s	0·002	0·0020	0·0020	0·0020	0·0020	0·0020	0·0021	0·0020	0·0021	0·0020	0·0020	0·0020
		(0·00002)	(0·00002)	(0·00007)	(0·00003)	(0·00002)	(0·00020)	(0·00003)	(0·00059)	(0·00003)	(0·00010)	(0·00003)
$u(0)$, m/s	100·0	99·995	99·996	99·993	99·996	100·072	99·974	100·004	99·951	100·192	100·136	98·955
		(0·141)	(0·141)	(0·144)	(0·143)	(1·098)	(0·153)	(0·279)	(0·206)	(1·549)	(1·423)	(28·660)
$w(0)$, m/s	10·0	10·003	10·004	10·003	10·001	10·012	10·014	9·892	10·505	10·021	10·016	10·001
		(0·032)	(0·036)	(0·034)	(0·083)	(0·063)	(0·045)	(3·928)	(0·466)	(0·097)	(0·083)	(0·085)
$\theta(0)$, rad	0·0	0·00002	0·00002	−0·00002	0·00003	0·00002	−0·00055	0·00003	0·00512	0·00003	0·00013	0·00003
		(0·00025)	(0·00028)	(0·00062)	(0·00028)	(0·00026)	(0·01080)	(0·00028)	(0·00459)	(0·00028)	(0·00086)	(0·00028)
rms(V)	—	0·0287	0·0287	0·0288	0·0286	0·243	0·0315	0·0284	0·0290	0·418	0·461	0·135
rms(α)	—	0·000165	0·000165	0·000165	0·000166	0·000156	0·000156	0·000642	0·00673	0·000153	0·000153	0·000699
rms(θ)	—	0·000165	0·000165	0·000168	0·000165	0·000166	0·000456	0·000165	0·00674	0·000165	0·000224	0·000165
rms(h)	—	0·0133	0·0163	0·0239	0·0105	0·0421	0·262	0·372	0·0125	0·1155	0·0117	0·0212

$N = 200$, record length = 20 s, R = diag[1·0, 250000, 250000, 0·1]fixed.
b_v, b_α, b_θ fixed at correct value.
Four iterations, typical CPU time about 60 s.
A priori parameter vector = $[0·0, 0·0, 0·0, 101·0, 10·3, 0·01]^T$.
Manoeuvre 1.

of the biases, a number of different procedures was tried as discussed in Section 2.4 and Appendix 3. Six methods used are summarised in the table below.

Method No.	Description
1	All nine parameters extracted as though independent
2	b_θ treated as function of $\theta(0)$
3	b_v, b_x, b_θ treated as functions of $u(0)$, $w(0)$, $\theta(0)$
4	$u(0)$, $w(0)$, $\theta(0)$ treated as functions of b_v, b_x, b_θ
5	b_v, b_x, b_θ, b_{ax} treated as functions of $u(0)$, $w(0)$, $\theta(0)$
6	$u(0)$, $w(0)$, $\theta(0)$ obtained from b_v, b_x, b_θ; sensitivities unchanged

Method 1 uses the unmodified sensitivities summarised in Appendix 1 while Methods 2–5 include modifications described in the corresponding sections of Appendix 3. Method 6 proceeds as in Method 1 but leaving out the initial conditions from the parameter vector. However, initial conditions are adjusted at each iteration using the relations in Section 2.4. Thus Method 6 is like Method 4 but without the sensitivity matrix elements being modified. This appears to be the approach used in Reference 9.

The manoeuvre used is the same as in the previous section (Manoeuvre 1) as are the fixed elements of the weighting matrix. Twenty seconds of record at 20 samples per second was analysed and typical computing time was 400 seconds for 20 iterations. For this and all subsequent computations the *a priori* values for the biases were set to zero and those for the initial conditions $u(0)$, $w(0)$ and $\theta(0)$ set to values determined from the "measurements".

A comparison of the performance of the six methods with noise free data is shown in Table 2. With Method 1, although the "Cramer–Rao" bounds are relatively small the estimated parameter values are clearly biased. Examination of the normalised correlation matrix reveals a number of highly correlated parameters, as expected, the worst being correlations between b_x–$w(0)$–$\theta(0)$ and between b_v–$u(0)$. An immediate improvement in parameter values is obtained with Method 2 when $\theta(0)$ is removed from the list of independent parameters. Further improvements are achieved with Methods 3 and 4 which give very similar results, as may be expected, but Method 5 shows little consistent improvement over the previous two methods. While estimated parameter values improve going from Method 1 to Method 5 it is worth noting that the confidence bounds for Methods 2–5 are worse than that of Method 1. Finally Method 6 is a poor performer giving strongly biased results. The "Cramer–Rao" bounds appear to be very small in this case but it should be remembered that the problem formulation is inconsistent.

3.3 Effect of Noise, Record Length and Sampling Rate

The effects of both measurement and process noise on the estimation procedures of the previous section were investigated using different (Gaussian) noise levels. Table 3 below lists the noise standard deviations on each of the measurement channels for five different noise levels used.

The first two columns in Table 3 are measurement noise only cases, the first column representing a fairly high noise level and the second a low noise level similar to that used in Reference 9. The last three columns include both process and measurement noise. Level 3 is a low process noise case (Ref. 9) confined with low measurement noise; Level 4 combines low process noise with high measurement noise and Level 5 has high noise levels in both process and measurement noise. Even the low noise levels in Table 3 are generally considerably higher than the levels described in Reference 10, which correspond to highly accurate instrumentation. Instrumentation of such accuracy is not yet in common use for flight testing.

TABLE 2

Comparison of Six Methods—No Noise

Parameter	True value	Method used					
		1	2	3	4	5	6
b_{ax}, m/s^2	0·1	0·167	0·109	0·098	0·098	0·119	0·188
		(0·0300)	(0·0760)	(0·0785)	(0·0784)	—	(0·0077)
b_{az}, m/s^2	0·1	0·112	0·101	0·097	0·097	0·100	0·115
		(0·0095)	(0·0143)	(0·0144)	(0·0144)	(0·0256)	(0·0038)
b_q, rad/s	0·002	0·0020	0·0020	0·0020	0·0020	0·0020	0·0020
		(0·00002)	(0·00001)	(0·00001)	(0·00001)	(0·00001)	(0·00002)
b_v, m/s	1·0	0·723	1·026	1·192	1·191	1·084	(0·736)
		(0·516)	(0·581)	—	(0·538)	—	(0·094)
b_x, rad	0·002	0·00062	0·00129	0·00228	0·00228	0·00206	−0·00405
		(0·00323)	(0·00322)	—	(0·0105)	—	(0·00022)
b_θ, rad	0·01	0·0028	0·0089	0·0103	0·0103	0·0081	−0·0001
		(0·0029)	—	—	(0·0082)	—	(0·0002)
$u(0)$, m/s	98·48	98·738	98·447	98·295	98·296	98·398	98·632
		(0·536)	(0·598)	(0·608)	—	(0·899)	—
$w(0)$, m/s	17·36	17·550	17·431	17·312	17·313	17·353	18·015
		(0·316)	(0·319)	(0·994)	—	(0·350)	—
$\theta(0)$, rad	0·175	0·182	0·176	0·174	0·174	0·176	0·185
		(0·0029)	(0·0078)	(0·0082)	—	(0·0147)	—
rms (V)	—	0·00418	0·00179	0·00158	0·00157	0·000495	0·03094
rms (α)	—	0·000056	0·000053	0·000059	0·000059	0·000757	0·000126
rms (θ)	—	0·000055	0·000055	0·000055	0·000055	0·000661	0·000055

N = 400, record length = 20 s, $\mathbf{R}$ = diag[1·0, 250000, 750000]fixed.
Only V, α, θ time histories matched
20 iterations, typical CPU time about 400 s.
A priori parameter vector = $[0·0, 0·0, 0·0, 0·0, 0·0, 0·0, 99·431, 17·734, 0·185]^T$.
Manoeuvre 1.

TABLE 3

Noise Levels

Standard error	Measurement noise only		Process and measurement noise		
	Level 1	Level 2	Level 3	Level 4	Level 5
$\sigma(ax)$, m/s^2	0·0	0·0	0·05	0·05	0·1
$\sigma(az)$, m/s^2	0·0	0·0	0·05	0·05	0·1
$\sigma(q)$, rad/s	0·0	0·0	0·001	0·001	0·002
$\sigma(V)$, m/s	1·0	0·1	0·1	1·0	1·0
$\sigma(\alpha)$, rad	0·002	0·001	0·001	0·002	0·002
$\sigma(\theta)$, rad	0·01	0·001	0·001	0·01	0·01

The effects of measurement noise on the results of the previous section are summarised in Table 4. The test details remain the same except that Level 1 noise has been added to the measurements and consequently the estimate for the measurement noise matrix, **R**, is updated in the course of the analysis as explained in Section 2.1. Thus the Cramer–Rao bound (equation 10) should be a good estimate of the accuracy of the estimates. The results in Table 4 represent the average values plus or minus the standard deviation (or scatter) obtained from 8 to 10 separate runs. The scatter should be comparable with the Cramer–Rao bounds shown in parentheses. In comparing Tables 2 and 4, the results for Method 1 (all parameters identified) are seen to be very similar. The scatter is about twice the Cramer–Rao bound for most parameters, indicating room for improvement. However, the mean values for all the parameters are within about one Cramer–Rao bound of their true value. The results from Method 6 remain erratic as before although apparently providing a reasonable fit. The Cramer–Rao bounds in this case give little indication of the accuracy of the estimated parameter values. The remaining methods all show a marked deterioration in the presence of measurement noise. The average results no longer compare favourably with those from Method 1 and the scatter bands are considerably worse. Method 4, not shown in Table 4, provides results very similar to Method 3. The deterioration in performance of Methods 2 to 5 in the presence of noise is probably linked to the fact, as discussed in Section 2.4, that the relations assumed by equation (23) no longer hold exactly.

It is concluded that, despite the correlations between several of the parameters, Method 1 is likely to provide the best results. In order to optimise further the performance of Method 1 the effects of record length, sampling time and measurement noise level have been examined and the results are shown in Table 5. These are average results over 7 to 10 simulations with the scatter and Cramer–Rao bound (in parentheses) also shown. Record lengths vary from 20 to 60 seconds and the number of samples, N, corresponds to sampling rates of either 20 or 40 samples per second. The first five columns of results are for Level 1 (high) measurement noise, the first (reference) column being a repeat of the Method 1 results from Table 4. Column 2 is for 40 seconds of record at the same sampling rate and shows a notable improvement in estimated parameters. The scatter of the results is much reduced and shows good agreement with the Cramer–Rao bounds in all cases. However, the scatter in some cases, in particular b_z, is still somewhat large. Doubling the sampling rate (column 3) produces further improvement in both estimates and scatter as does an increase in the record length from 40 to 60 seconds (column 4) at the lower sampling rate. Column 5 gives results for 60 seconds of record at the higher (40 per second) sampling rates. The improving results with increasing record length are partly due to decreasing correlations between parameters, but close examination of the results suggests that there may still be some bias in b_{ax} and perhaps also $\theta(0)$.

The last two columns of Table 5 are for lower (level 2) measurement noise. As expected results are improved for both estimated values and scatter. At this noise level 40 seconds of record is sufficient to identify all the biases to within about 10% or better.

The addition of process noise can be expected to affect the results adversely, since it has not been accounted for, and some results are shown in Table 6. These can be compared directly with the relevant columns of Table 5. For example columns 1 and 2 of Table 6 should be compared

TABLE 4

Effect of Measurement Noise Using Different Methods

Parameter	True value	Method used				
		1	2	3	5	6
b_{ax}, m/s^2	0·1	0·167 ± 0·126 (0·0686)	0·177 ± 0·170 (0·0757)	−0·008 ± 0·243 (0·0786)	—	0·118 ± 0·088 (0·0125)
b_{az}, m/s^2	0·1	0·115 ± 0·028 (0·0150)	0·116 ± 0·033 (0·0148)	0·082 ± 0·042 (0·0139)	0·136 ± 0·185 (0·0248)	0·114 ± 0·012 (0·00765)
b_q, rad/s	0·002	0·0020 ± 0·00004 (0·00008)	0·0020 ± 0·00003 (0·00001)	0·0020 ± 0·00005 (0·00004)	0·0020 ± 0·00004 (0·00004)	0·0020 ± 0·00008 (0·00008)
b_v, m/s	1·0	0·625 ± 1·069 (0·573)	0·563 ± 1·107 (0·580)	—	—	0·563 ± 0·700 (0·099)
b_z, rad	0·002	0·0024 ± 0·0099 (0·0032)	−0·0033 ± 0·0074 (0·0032)	—	—	−0·0032 ± 0·0030 (0·0002)
b_θ, rad	0·01	0·0031 ± 0·0133 (0·0070)	—	—	—	0·0067 ± 0·0096 (0·0009)
$u(0)$, m/s	98·48	98·866 ± 1·071 (0·588)	98·865 ± 1·142 (0·598)	98·871 ± 1·484 (0·610)	98·654 ± 3·734 (0·919)	—
$w(0)$, m/s	17·36	17·382 ± 0·987 (0·316)	17·966 ± 0·725 (0·320)	17·072 ± 0·958 (0·991)	17·631 ± 0·714 (0·440)	—
$\theta(0)$, m/s	0·175	0·181 ± 0·014 (0·0070)	0·184 ± 0·018 (0·0078)	0·163 ± 0·025 (0·0082)	0·183 ± 0·074 (0·0150)	—
rms (V)	—	1·048	0·993	1·024	0·998	1·065
rms (α)	—	0·00215	0·00180	0·00198	0·00198	0·00188
rms (θ)	—	0·00962	0·01023	0·0102	0·00987	0·00952

Level 1 (measurement) noise.
N = 400, record length = 20 s.
Only V, α, θ records matched; $\mathbf{R}$ = diag[1·0, 250000, 10000] initially.
20 iterations, typical CPU time about 400 s.
A priori parameter vector = $[0·0, 0·0, 0·0, 0·0, 0·0, 0·0, 0·0, 99·431, 17·734, 0·185]^T$.
Results are averages of 8–10 runs.
Manoeuvre 1.

TABLE 5

Effect of Record Length, Sampling Rate and Measurement Noise Level—Method 1

Parameter	True value	Level 1 measurement noise					Level 2 measurement noise	
		1	2	3	4	5	6	7
b_{ax}, m/s²	0·1	0·167±0·126 (0·0686)	0·129±0·017 (0·0175)	0·115±0·013 (0·0123)	0·090±0·007 (0·0072)	0·087±0·005 (0·0051)	0·110±0·003 (0·0033)	0·104±0·001 (0·0019)
b_{az}, m/s²	0·1	0·115±0·0283 (0·0150)	0·105±0·0064 (0·0055)	0·102±0·0032 (0·0039)	0·100±0·0020 (0·0027)	0·099±0·0017 (0·0019)	0·100±0·0017 (0·0011)	0·099±0·0004 (0·0005)
b_q, rad/s	0·002	0·0020±0·00004 (0·00008)	0·0020±0·000022 (0·00002)	0·0020±0·00002 (0·00002)	0·0020±0·00001 (0·00001)	0·0020±0·00001 (0·00001)	0·0020±0·000002 (0·000002)	0·0020±0·000001 (0·000001)
b_v, m/s	1·0	0·6254±1·0694 (0·5732)	0·7484±0·3500 (0·3208)	0·9338±0·1925 (0·2260)	0·9962±0·1036 (0·1905)	0·9611±0·0851 (0·1331)	1·0237±0·0875 (0·0548)	1·0329±0·0160 (0·0238)
b_x, rad	0·002	0·00244±0·0099 (0·0032)	0·0008±0·0014 (0·0018)	0·0017±0·0012 (0·0012)	0·0022±0·0010 (0·0009)	0·0014±0·0005 (0·0006)	0·0018±0·0002 (0·0004)	0·0017±0·0002 (0·0002)
b_θ, rad	0·01	0·0031±0·0133 (0·0070)	0·0065±0·0014 (0·0018)	0·0084±0·0013 (0·0013)	0·0111±0·0006 (0·0008)	0·0112±0·0006 (0·0006)	0·0090±0·0004 (0·0003)	0·0096±0·0001 (0·0002)
$u(0)$, m/s	98·48	98·866±1·071 (0·588)	98·729±0·360 (0·333)	98·557±0·172 (0·234)	98·500±0·149 (0·208)	98·564±0·094 (0·147)	98·451±0·092 (0·056)	98·444±0·018 (0·026)
$w(0)$, m/s	17·36	17·382±0·987 (0·316)	17·521±0·161 (0·196)	17·408±0·123 (0·138)	71·337±0·116 (0·103)	17·439±0·051 (0·073)	17·382±0·027 (0·044)	17·388±0·022 (0·020)
$\theta(0)$, m/s	0·175	0·181±0·014 (0·0070)	0·178±0·0015 (0·0018)	0·176±0·0015 (0·0013)	0·173±0·0004 (0·0007)	0·173±0·0005 (0·0005)	0·176±0·0004 (0·0003)	0·175±0·0001 (0·0002)
rms (V)	—	1·048	1·024	1·038	1·010	0·981	0·1011	0·0981
rms (α)	—	0·00215	0·00202	0·00197	0·00195	0·00196	0·000986	0·000975
rms (θ)	—	0·00962	0·00978	0·00992	0·00962	0·00993	0·000999	0·001004
Length, s	—	20	40	40	60	60	40	60
N	—	400	800	1600	1200	2400	1600	2400

Only V, α, θ records matched; $\mathbf{R}$ = diag[1·0, 250000, 10000] initially.
10 iterations (except case 1 has 20); CPU time for cases 5 and 7 typically 20 min for 10 iterations.
A priori parameter vector, $[0·0, 0·0, 0·0, 0·0, 0·0, 0·0, 99·4310, 17·7340, 0·1845]^T$.
Results are averages of 7–10 runs.
Manoeuvre 1.

with columns 7 and 5, respectively, of Table 5. While the respective Cramer–Rao bounds remain the same, the scatter increases markedly. This deterioration is relatively much worse in the case with low measurement noise (column 1). Nevertheless most of the biases are reasonably well identified when 60 seconds of record are used, the main exception being b_x which has a large scatter band. When either the record length is decreased (column 3) or the level of process noise is increased (column 4) the accuracy of estimation of several of the other parameters also becomes unacceptable, but it is clear that b_q is always well identified followed probably by b_{az}.

TABLE 6

Effect of Process and Measurement Noise—Method 1

Parameter	True value	1	2	3	4
b_{ax}, m/s^2	0·1	0·086±0·006 (0·0020)	0·087±0·011 (0·0051)	0·051±0·020 (0·0125)	0·089±0·021 (0·0053)
b_{az}, m/s^2	0·1	0·099±0·005 (0·0005)	0·095±0·003 (0·0019)	0·092±0·011 (0·0039)	0·092±0·008 (0·0020)
b_q, rad/s	0·002	0·0020±0·00002 (0·000001)	0·0020±0·00002 (0·00001)	0·0020±0·00005 (0·00002)	0·0020±0·00005 (0·00001)
b_v, m/s	1·0	1·038±0·134 (0·025)	1·132±0·163 (0·135)	1·213±0·526 (0·230)	1·234±0·479 (0·138)
b_x, rad	0·002	0·0019±0·0015 (0·0002)	0·0018±0·0026 (0·0006)	0·0052±0·0029 (0·0013)	0·00017±0·0034 (0·0006)
b_θ, rad	0·01	0·0114±0·0004 (0·0002)	0·0115±0·0011 (0·0006)	0·0158±0·0023 (0·0013)	0·0111±0·0021 (0·0006)
$u(0)$, m/s	98·48	98·436±0·172 (0·026)	98·315±0·197 (0·147)	98·303±0·520 (0·238)	98·219±0·556 (0·150)
$w(0)$, m/s	17·36	17·360±0·161 (0·020)	17·379±0·306 (0·073)	17·028±0·340 (0·140)	17·505±0·354 (0·075)
$\theta(0)$, rad	0·175	0·173±0·001 (0·0002)	0·1728±0·001 (0·0005)	0·1690±0·002 (0·0013)	0·1731±0·002 (0·0005)
Time, sec	—	60	60	40	60
N	—	2400	2400	1600	2400
Noise	—	Level 3	Level 4	Level 4	Level 5

Only V, α, θ records matched; $\mathbf{R}$ = diag[1·0, 250000, 10000] initially.
10 iterations—CPU time about 20 min for cases 1, 2, 4 and 14 min for case 3.
A priori parameter vector = $[0·0, 0·0, 0·0, 0·0, 0·0, 0·0, 99·431, 17·734, 0·185]^T$.
Results averages of seven runs.
Manoeuvre 1.

3.4 Effect of Manoeuvre Shape

All of the results so far presented were obtained using the manoeuvre shape (Manoeuvre 1) shown in Figure 2. It is known that manoeuvre shape influences the amount of information in the measurements and efforts have been made elsewhere in the development of optimal manoeuvre shapes (see e.g. Ref. 15). No attempt is made here to develop an optimal shape but in this Section results with changing manoeuvre shapes are reported so as to bring out the effect this can have on the results.

The shapes used are as follows:

Manoeuvre 1.—Shown in Figure 2, the inputs consist of a longitudinal deceleration at 0·1 m/s^2, an oscillatory normal acceleration with an amplitude of 2 m/s^2 and an oscillatory pitch rate with an amplitude of 0·2 rad. The frequency of oscillation in each case is 2 rad/s.

TABLE 7

Effect of Manoeuvre Shape–Method 1

Parameter	True value	Manoeuvre shape						
		1	2	3	4	5	5	5
b_{ax}, m/s^2	0·1	0·115±0·013 (0·0124)	0·013 (0·0237)	0·037 (0·0217)	0·116 (0·0172)	0·090 (0·0079)	0·089±0·025 (0·0080)	0·104±0·008 (0·0018)
b_{az}, m/s^2	0·1	0·102±0·003 (0·0038)	0·094 (0·0025)	0·095 (0·0024)	0·098 (0·0022)	0·101 (0·0025)	0·101±0·007 (0·0025)	0·101±0·003 (0·0004)
b_q, rad/s	0·002	0·0020±0·00002 (0·00002)	0·0020 (0·00002)	0·0020 (0·00002)	0·0020 (0·00002)	0·0020 (0·00002)	0·0020±0·00004 (0·00002)	0·0020±0·00004 (0·000002)
b_v, m/s	1·0	0·934±0·193 (0·226)	0·586 (0·323)	0·920 (0·127)	0·987 (0·057)	1·003 (0·039)	0·942±0·092 (0·039)	0·978±0·084 (0·014)
b_x, rad	0·002	0·0017±0·0012 (0·0012)	0·0014 (0·0008)	0·0024 (0·0007)	0·0022 (0·0008)	0·0031 (0·0008)	0·0030±0·0017 (0·0008)	0·0020±0·0003 (0·0001)
b_θ, rad	0·01	0·0084±0·0013 (0·0013)	0·0186 (0·0024)	0·0165 (0·0022)	0·0082 (0·0018)	0·0110 (0·0009)	0·115±0·0030 (0·0009)	0·0096±0·0009 (0·0002)
$u(0)$, m/s	98·48	98·557±0·172 (0·234)	98·946 (0·317)	98·589 (0·136)	98·434 (0·082)	98·479 (0·064)	98·513±0·146 (0·064)	98·502±0·097 (0·015)
$w(0)$, m/s	17·36	17·408±0·123 (0·138)	17·470 (0·116)	17·302 (0·080)	17·333 (0·077)	17·240 (0·081)	17·289±0·143 (0·082)	17·392±0·059 (0·012)
$\theta(0)$, rad	0·175	0·176±0·001 (0·0015)	0·166 (0·0024)	0·168 (0·0022)	0·175 (0·0017)	0·174 (0·0009)	0·174±0·003 (0·0009)	0·175±0·001 (0·0002)
rms (V)		1·038	0·966	0·982	0·990	0·993	0·971	0·104
rms (α)		0·00197	0·00202	0·00194	0·00198	0·00205	0·00210	0·00104
rms (θ)		0·00992	0·00966	0·01000	0·00981	0·01016	0·00989	0·00102
Noise		Level 1	Level 1	Level 1	Level 1	Level 1	Level 5	Level 3

Only V, α, θ records matched, $\mathbf{R}$ = diag[1·0, 250000, 10000] initially.
N = 1600, time = 40 s, 10 iterations.
A priori values: biases = 0·0, initial conditions from measurements.
Results with process noise are average of nine runs.

Manoeuvre 2.—Shown in Figure 4, the only difference from the previous inputs being in the normal acceleration which has now been made symmetrical about the undisturbed value. The output airspeed, incidence and attitude are shown in Figure 5. Level 1 (measurement) noise is shown on the outputs and the calculations assume zero biases. Thus the differences between the two sets of curves represent the effects of the biases. The major difference between this and the previous manoeuvre is in the angle of attack which no longer reaches the very high values caused by the asymmetric normal acceleration input.

Manoeuvre 3.—This manoeuvre is very similar to the previous except that the normal acceleration amplitude has been increased to 10 m/s^2 thus providing a wider range in angle of attack.

Manoeuvre 4 (Fig. 6).—This manoeuvre differs from the previous only in having a different oscillation frequency for the input normal acceleration. The differences in the output records are shown in Figure 7.

Manoeuvre 5 (Fig. 8).—This is a simulation of a real manoeuvre produced by a pilot applying stick inputs to produce a roller coaster type of motion, i.e. push-over/pull-up/push-over. The resulting accelerations and pitch rate are similar to those shown in Figure 8, with the higher frequency oscillations, particularly in pitch but also in normal acceleration, being due to the Short Period response. The outputs, both measured (with Level 1 noise) and calculated (assuming zero biases) are shown in Figure 9.

The results using these five manoeuvre shapes are shown in Table 7. For this study 40 seconds of record at 40 samples per second were used. Consider first the five columns of results with Level 1 measurement noise only. For Manoeuvre 1 the results are a repeat of those in Table 5, column 3. With Manoeuvre 2 the smaller angle of attack range leads to a general worsening of results, both in parameter value and Cramer–Rao bound. Of the biases, only b_q and perhaps b_{az} can be taken as satisfactorily identified. With Manoeuvre 3 the larger disturbance amplitude produces a general improvement in results all round. However, b_θ and b_{ax} still are strongly biased as indicated by the Cramer–Rao bounds. Manoeuvre 4 introduces two dominant frequencies, particularly obvious in the angle of attack output (Fig. 7), and this extra information leads to a further general improvement in the parameter estimates and error bounds. In addition biases in b_{ax} and b_θ are no longer obvious. Finally, the information content of Manoeuvre 5 is such as to produce the best results in this Section. Only b_α (and the related initial value, $w(0)$) still appear troublesome.

The last two columns of Table 7 include both process and measurement noise with Manoeuvre 5. The Level 5 (high process and measurement noise) results are, on average, very similar to the measurement noise only (Level 1) case although the scatter, based on the standard deviation over nine runs, is two to three times worse than the Cramer–Rao bound now. The Level 3 (low process and measurement noise) results produce a marked improvement with all parameters being well identified. Although the scatter is about five times the Cramer–Rao bound, it is comparable and in some cases better than the Cramer–Rao bounds obtained with the higher levels of measurement noise. In particular b_α and $w(0)$ are considerably improved.

3.5 Summary of Results

The results for the longitudinal kinematic system studied here have suggested that the use of the three elements V, α, θ of the output vector produce results as good as those using the full vector, including height. Reduced computation time and simplicity also favour a reduced system.

The problem of correlations between the state initial conditions and some parameters was investigated using several possible methods proposed to account for the correlations. Although improved performance was obtained from these methods in the noise free case, the addition of measurement noise led to marked deterioration. Best results, with measurement noise, were obtained when all parameters including initial conditions were independently extracted.

Correlations decreased as record lengths increased with consequent decrease in the bias in some estimates and decrease in the scatter band. Reasonable accuracy could be obtained with a record length of 40 seconds at 40 samples per second. Reduction of measurement noise levels was also found to lead to marked improvement in parameter estimates. The main effect of process noise was an increase in the scatter of results. Also bias in some estimates appeared where previously absent with measurement noise alone.

It was clear that the manoeuvre shape had an important influence on the results. A practical push-over/pull-up manoeuvre was found to provide satisfactory results for most parameters with a record length of 40 seconds, particularly for lower noise levels (both measurement and process). Further improvements may well be attainable by developing a manoeuvre specially suited to the purpose of identifying instrument biases.

4. CONCLUSIONS

A general Maximum Likelihood program, suitable for estimation of parameters in non-linear systems, has been described. For successful application to a particular system, process noise levels should be small. A summary of the theoretical background has been given and the program structure has been developed via subroutines to allow ready modification to suit the problem in hand.

The program has been applied here to a study involving longitudinal aircraft kinematics. In this case the kinematic equations, treated separately from a dynamic representation of aircraft motions, are free from process noise to a good approximation. This separate treatment of the kinematics can be used for checking the compatibility of measurements and for estimating instrument systematic errors. Such an approach is useful for reconstructing "error-free" records prior to dynamic analysis aimed at estimating aerodynamic parameters, and is particularly valuable when the dynamic model is uncertain and/or non-linear.

The study, using simulated data, has aimed at establishing the conditions under which the Maximum Likelihood algorithm can successfully extract the instrument biases, and to set a baseline for comparison with other methods. It has been found that the present method is feasible provided record lengths and sampling rates are adequate. The importance of using high quality instrumentation to minimise noise has also been brought out. Further, it has been shown that the manoeuvre shape can have a considerable influence on the quality of results and an effort to develop an optimal manoeuvre shape may be worthwhile. For the present system, using a practical manoeuvre shape, 40 seconds of record at 40 samples a second with reasonably low measurement and process noise levels was successful in extracting most parameters to within 10% or better of their true values. The precise levels of accuracy acceptable would depend, to some extent, on the requirements of the subsequent analysis and would need to be investigated further. Finally, the performance needs to be checked with real, as opposed to simulated, flight test data.

REFERENCES

1. Feik, R. A.: Transonic Pitch Damping of a Delta Wing Aircraft Determined from Flight Measurements. ARL, Aero. Report 153, July 1979.

2. Maine, R. E., and Iliff, K.: Formulation and Implementation of a Practical Algorithm for Parameter Estimation with Process and Measurement Noise. Atmos. Flight Mechanics Conference, Danvers, Mass., August 1980.

3. High Angle of Attack Aerodynamics. AGARD Conference Proceedings No. 247, October 1978.

4. Vincent, J. H., Gupta, N. K., and Hall, W. E.: Recent Results in Parameter Identification for High Angle-of-Attack Stall Regimes. Atmos. Flight Mechanics Conference, Boulder, Colo., August 1979.

5. Klein, V.: Identification Evaluation Methods. AGARD Lecture Series 104, October 1979.

6. Jonkers, H. L.: Application of the Kalman Filter to Flight Path Reconstruction from Flight Test Data including Estimation of Instrumental Bias Error Corrections. Doctoral Thesis, Delft Univ. of Technology, February 1976.

7. Klein, V., and Schiess, J. R.: Compatibility Check of Measured Aircraft Responses Using Kinematic Equations and Extended Kalman Filter. NASA TN D-8514, August 1977.

8. Martin, C. A.: Estimation of Aircraft Dynamic States and Instrument Systematic Errors from Flight Test Measurements Using the Carlson Square Root Formulation of the Kalman Filter. ARL, Aero. Note 399, September 1980.

9. Keskar, D. A., and Klein, V.: Determination of Instrumentation Errors from Measured Data Using Maximum Likelihood Method. Atmos. Flight Mechanics Conference, Danvers, Mass., August 1980.

10. Horsten, J. J., Jonkers, H. L., and Mulder, J. A.: Flight Path Reconstruction in the Context of Nonsteady Flight Testing. Delft Univ. of Technology Report LR-280, May 1979.

11. Goodwin, G. C., and Payne, R. L.: *Dynamic System Identification: Experiment Design and Data Analysis*. Academic Press, 1977.

12. Taylor, L. W., and Iliff, K. W.: Systems Identification Using a Modified Newton-Raphson Method—A Fortran Program. NASA TN D-6734, May 1972.

13. Etkin, B.: *Dynamics of Atmospheric Flight*. John Wiley and Sons, 1972.

14. Shampine, L. F., and Gordon, M. K.: Using DE/Step, Intrp to Solve Ordinary Differential Equations. Sandia Laboratories, SAND-75-0211, April 1975.

15. Garretson, H. C., III: Beaver Aircraft Parameter Identification—Technical Preparations and Preliminary Results. DFVLR-Mitt. 78-01, 1978.

APPENDIX 1

Sensitivity Matrix (Subroutine SENS)

The parameter vector has dimension 9:

$$\xi = [b_{ax}, b_{az}, b_q, b_v, b_\alpha, b_\theta, u(0), w(0), \theta(0)]^T$$

and the output vector has dimension 4:

$$z_\xi = [V_{out}, \alpha_{v_{out}}, \theta_{out}, h_{out}]^T.$$

Using the output definition in equation (15), the transpose of the 4×9 sensitivity matrix becomes:

$z_\xi \rightarrow$ ξ $\downarrow$	V_{out}	$\alpha_{v_{out}}$	θ_{out}	h_{out}
b_{ax}	$V_{out,b_{ax}}$	$\alpha_{v_{out},b_{ax}}$	0·0	$h_{out,b_{ax}}$
b_{az}	$V_{out,b_{az}}$	$\alpha_{v_{out},b_{az}}$	0·0	$h_{out,b_{az}}$
b_q	V_{out,b_q}	α_{v_{out},b_q}	θ_{out,b_q}	h_{out,b_q}
b_v	1·0	0·0	0·0	0·0
b_α	0·0	1·0	0·0	0·0
b_θ	0·0	0·0	1·0	0·0
$u(0)$	$V_{out,u(0)}$	$\alpha_{v_{out},u(0)}$	0·0	$h_{out,u(0)}$
$w(0)$	$V_{out,w(0)}$	$\alpha_{v_{out},w(0)}$	0·0	$h_{out,w(0)}$
$\theta(0)$	$V_{out,\theta(0)}$	$\alpha_{v_{out},\theta(0)}$	$\theta_{out,\theta(0)}$	$h_{out,\theta(0)}$

where

$$V_{out,\xi_j} = (u \cdot u_{\xi_j} + w \cdot w_{\xi_j})/(u^2+w^2)^{1/2},$$

$$\alpha_{v_{out},\xi_j} = (u \cdot w_{\xi_j} - [w-(q_m+b_q)x_\alpha]u_{\xi_j})/(u^2+[w-(q_m+b_q)x_\alpha]^2),$$

$$\theta_{out,\xi_j} = \theta_{\xi_j},$$

$$h_{out,\xi_j} = h_{\xi_j}.$$

The above relations hold for those elements ξ_j of the parameter vector as listed above in the sensitivity matrix. The only exception is

$$\alpha_{v_{out},b_q} = (u \cdot w_{b_q} - [w-(q_m+b_q)x_\alpha]u_{b_q} - u \cdot x_\alpha)/(u^2+[w-(q_m+b_q)x_\alpha]^2).$$

APPENDIX 2

Differential Equations (Subroutine DERIVS)

In order to calculate the state (equation (14)) and the elements of the sensitivity matrix (Appendix 1) the following system of ordinary differential equation needs to be integrated with respect to time:

$$\dot{u} = -(q_m+b_q)w+(ax_m+b_{ax})-g\sin\theta$$

$$\dot{w} = (q_m+b_q)u+(az_m+b_{az})+g\cos\theta$$

$$\dot{\theta} = q_m+b_q$$

$$\dot{h} = u\sin\theta-w\cos\theta$$

$$\dot{u}_{b_{ax}} = -(q_m+b_q)w_{b_{ax}}+1$$

$$\dot{w}_{b_{ax}} = (q_m+b_q)u_{b_{ax}}$$

$$\dot{h}_{b_{ax}} = \sin\theta\,.\,u_{b_{ax}}-\cos\theta\,.\,w_{b_{ax}}$$

$$\dot{u}_{b_{az}} = -(q_m+b_q)w_{b_{az}}$$

$$\dot{w}_{b_{az}} = (q_m+b_q)u_{b_{az}}+1$$

$$\dot{h}_{b_{az}} = \sin\theta\,.\,u_{b_{az}}-\cos\theta\,.\,w_{b_{az}}$$

$$\dot{u}_{b_q} = -(q_m+b_q)w_{b_q}-w-g\cos\theta\,.\,\theta_{b_q}$$

$$\dot{w}_{b_q} = (q_m+b_q)u_{b_q}+u-g\sin\theta\,.\,\theta_{b_q}$$

$$\dot{\theta}_{b_q} = 1\cdot 0$$

$$\dot{h}_{b_q} = \sin\theta\,.\,u_{b_q}-\cos\theta\,.\,w_{b_q}+(u\cos\theta+w\sin\theta)\theta_{b_q}$$

$$\dot{u}_{u(0)} = -(q_m+b_q)w_{u(0)}$$

$$\dot{w}_{u(0)} = (q_m+b_q)u_{u(0)}$$

$$\dot{h}_{u(0)} = \sin\theta\,.\,u_{u(0)}-\cos\theta\,.\,w_{u(0)}$$

$$\dot{u}_{w(0)} = -(q_m+b_q)w_{w(0)}$$

$$\dot{w}_{w(0)} = (q_m+b_q)u_{w(0)}$$

$$\dot{h}_{w(0)} = \sin\theta\,u_{w(0)}-\cos\theta\,.\,w_{w(0)}$$

$$\dot{u}_{\theta(0)} = -(q_m+b_q)w_{\theta(0)}-g\cos\theta$$

$$\dot{w}_{\theta(0)} = (q_m+b_q)u_{\theta(0)}-g\sin\theta$$

$$\dot{h}_{\theta(0)} = \sin\theta\,.\,u_{\theta(0)}-\cos\theta\,.\,w_{\theta(0)}+u\cos\theta+w\sin\theta$$

In deriving these equations use has been made of the fact that $\theta_{\theta(0)} = 1$. The initial conditions for the above set of equations are zero except for the following:

$$\left.\begin{array}{l} u(0) \\ w(0) \\ \theta(0) \end{array}\right\} \text{unknown parameters to be estimated}$$

$$u_{u(0)}(0) = 1$$

$$w_{w(0)}(0) = 1$$

APPENDIX 3

Effect of Correlations on Sensitivity Matrix

As explained in Section 2.4, when relationships between initial conditions and biases are accounted for, it is possible to reduce the number of parameters to be estimated. At the same time, alterations need to be made to some elements of the sensitivity matrix defined in Appendix 1. Four possible approaches which have been examined and the resulting changed elements of the sensitivity matrix are summarised below.

(1) Parameter vector, $[b_{ax},b_{az},b_q,b_v,b_x,u(0),w(0),\theta(0)]^T - b_\theta$ treated as a function of $\theta(0)$.

Changed sensitivity elements:

$$\theta_{out,\theta(0)} = 0$$

(2) Parameter vector, $[b_{ax},b_{az},b_q,u(0),w(0),\theta(0)]^T - b_v,b_\alpha,b_\theta$ treated as functions of $u(0)$, $w(0)$, $\theta(0)$.

Changed sensitivity elements:

$$V_{out,u(0)} = (u \cdot u_{u(0)} + w \cdot w_{u(0)})(/u^2+w^2)^{1/2} - u(0)/(u^2(0)+w^2(0))^{1/2}$$

$$V_{out,w(0)} = (u \cdot u_{w(0)} + w \cdot w_{w(0)})/(u^2+w^2)^{1/2} - w(0)/u^2(0)+w^2(0))^{1/2}$$

$$\alpha_{v_{out},u(0)} = (u \cdot w_{u(0)} - [w-(q_m+b_q)x_\alpha]u_{u(0)})/(u^2+[w-(q_m+b_q)x_\alpha]^2)$$
$$+(w(0)-(q_m+b_q)x_\alpha)/(u^2(0)+[w(0)-(q_m(0)+b_q)x_\alpha]^2)$$

$$\alpha_{v_{out},w(0)} = (u \cdot w_{w(0)} - [w-(q_m+b_q)x_\alpha]u_{w(0)})/(u^2+[w-(q_m+b_q)x_\alpha]^2)$$
$$-u(0)/(u^2(0)+[w(0)-(q_m(0)+b_q)x_\alpha]^2)$$

$$\theta_{out,\theta(0)} = 0$$

(3) Parameter vector, $[b_{ax},b_{az},b_q,b_v,b_x,b_\theta]^T - u(0),w(0),\theta(0)$ treated as functions of b_v, b_α, b_θ

Changed sensitivity elements:

$$V_{out,b_v} = 1 - -[(u \cdot u_{u(0)} + w \cdot w_{u(0)})\cos\alpha(0)$$
$$+(u \cdot u_{w(0)} + w \cdot w_{w(0)})\sin\alpha(0)]/(u^2+w^2)^{1.2}$$

$$V_{out,b_x} = [(u \cdot u_{u(0)} + w \cdot w_{u(0)})\sin\alpha(0)$$
$$-(u \cdot u_{w(0)} + w \cdot w_{w(0)})\cos\alpha(0)] \cdot (u^2(0)+w^2(0))^{1\ 2}/(u^2+w^2)^{1\ 2}$$

$$V_{out,b_\theta} = -(u \cdot u_{\theta(0)} + w \cdot w_{\theta(0)})/(u^2+w^2)^{1\ 2}$$

$$\alpha_{v_{out},b_v} = [(w \cdot u_{u(0)} - u \cdot w_{u(0)})\cos\alpha(0) + (w \cdot u_{w(0)} - u \cdot w_{w(0)})\sin\alpha(0)]/(u^2+w^2)$$

$$\alpha_{v_{out},b_x} = 1 + [(u \cdot w_{u(0)} - w \cdot u_{u(0)})\sin\alpha(0) +$$
$$+(w \cdot u_{w(0)} - u \cdot w_{w(0)})\cos\alpha(0)] \cdot (u^2(0)+w^2(0))^{1\ 2}/(u^2+w^2)$$

$$\alpha_{v_{out},b_\theta} = (w \cdot u_{\theta(0)} - u \cdot w_{\theta(0)})/(u^2+w^2)$$

$$\theta_{out,b_\theta} = 0$$

These relations assume initially steady flight, i.e. pitch rate equals zero.

(4) Parameter vector, $[b_{az},b_q,u(0),w(0),\theta(0)]-b_v,b_\alpha,b_\theta$ and b_{ax} treated as functions of $u(0)$, $w(0)$, $\theta(0)$.

Changed sensitivity elements:

$V_{out,u(0)}$, $V_{out,w(0)}$, $\alpha_{v_{out},u(0)}$, $\alpha_{v_{out},w(0)}$ and $\theta_{out,\theta(0)}$ same as listed in approach 2. In addition:

$$V_{out,\theta(0)} = [u \,.\, u_{\theta(0)}+w \,.\, w_{\theta(0)}-(az_m(0)+b_{az})\sec^2\theta(0)(u \,.\, u_{b_{ax}}+w \,.\, w_{b_{ax}})]/(u^2+w^2)^{1/2}$$

$$\alpha_{v_{out},\theta(0)} = [u \,.\, w_{\theta(0)}-w \,.\, u_{\theta(0)}-(az_m(0)+b_{az})\sec^2\theta(0)(u \,.\, w_{b_{ax}}-w \,.\, u_{b_{ax}})]/(u^2+w^2)$$

Initially steady flight, i.e. zero pitch rate, has been assumed in these relations.

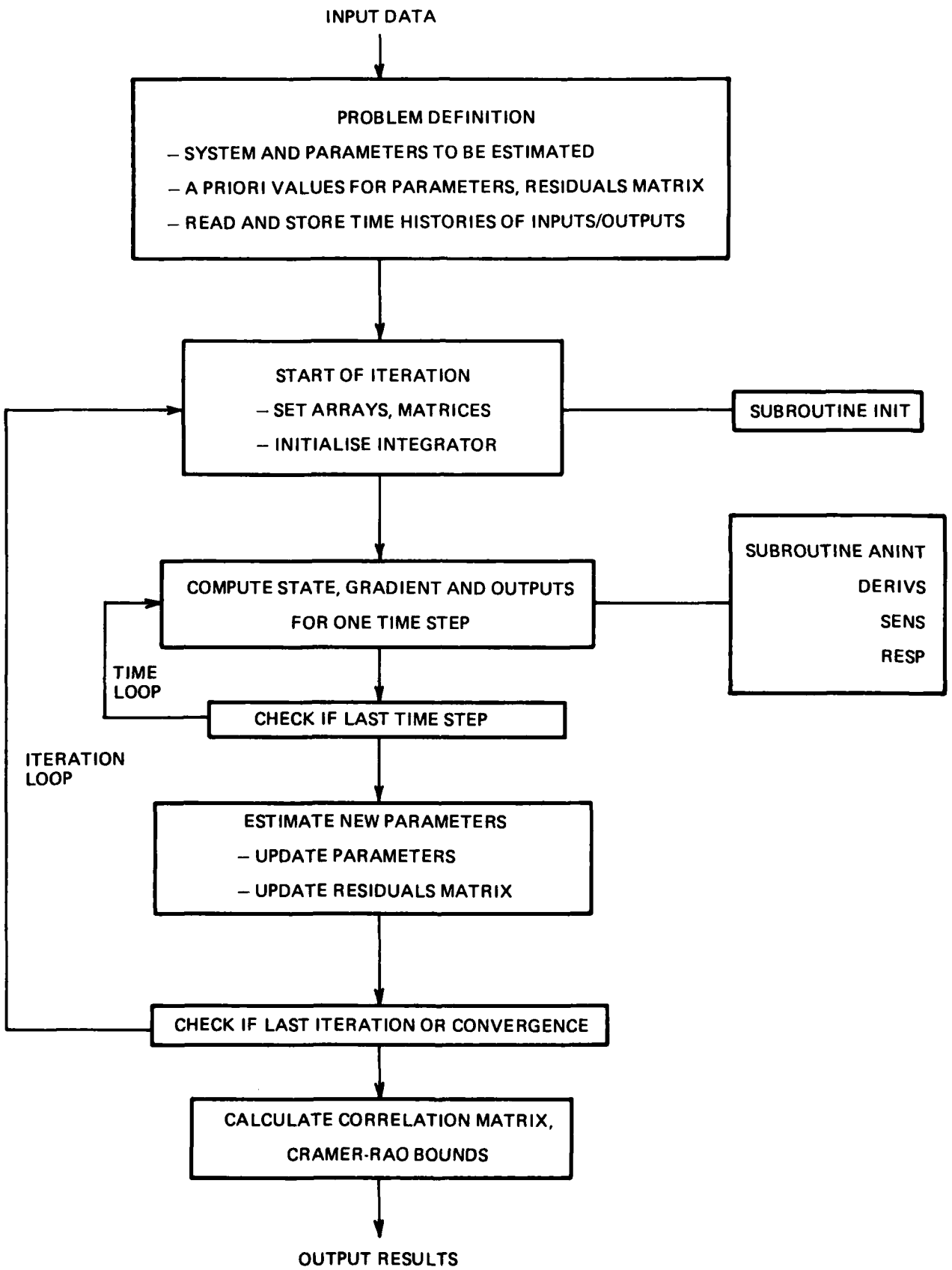

FIG. 1 BASIC PROGRAM STRUCTURE

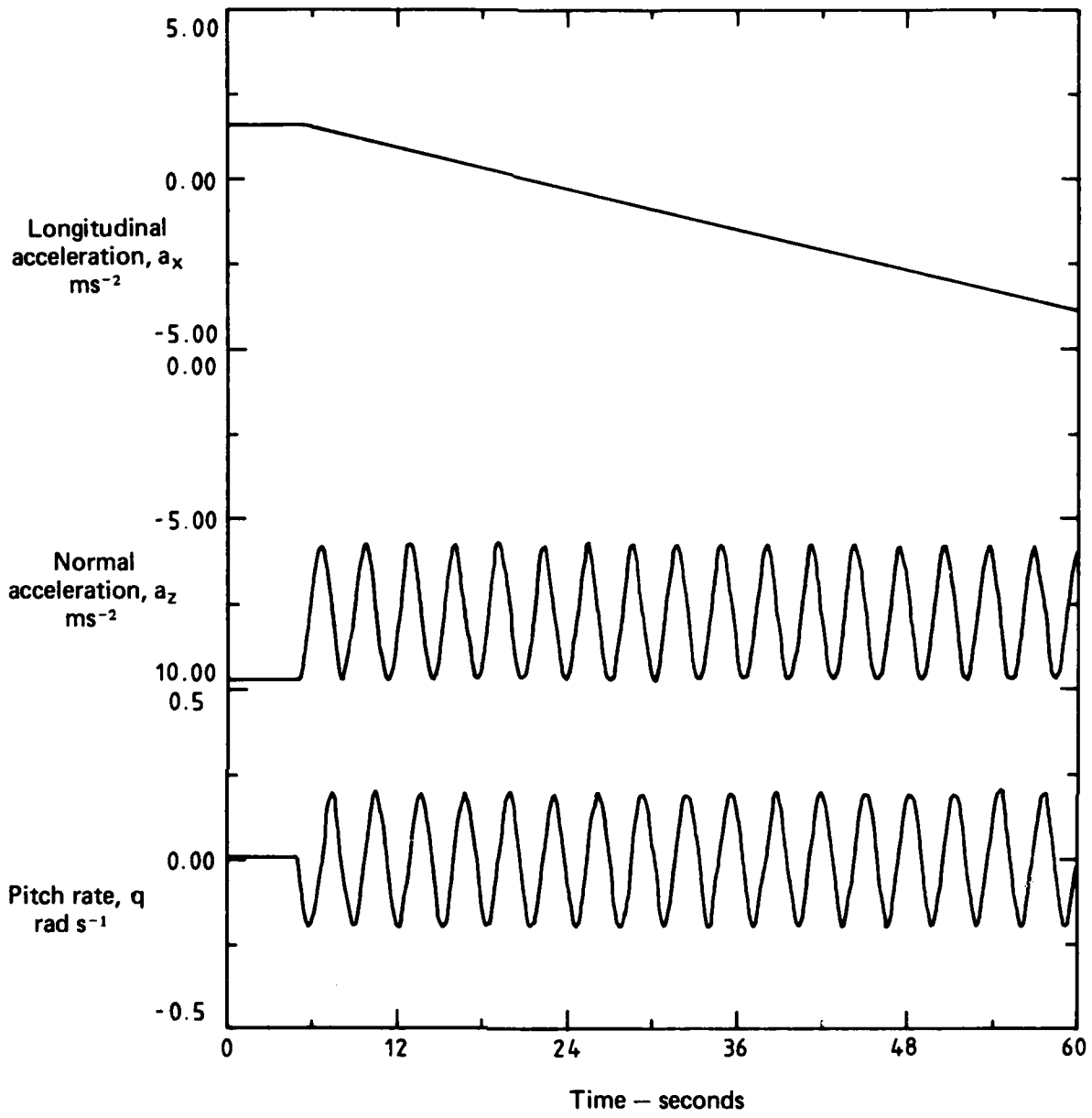

FIG. 2 MANOEUVRE 1 -- INPUTS

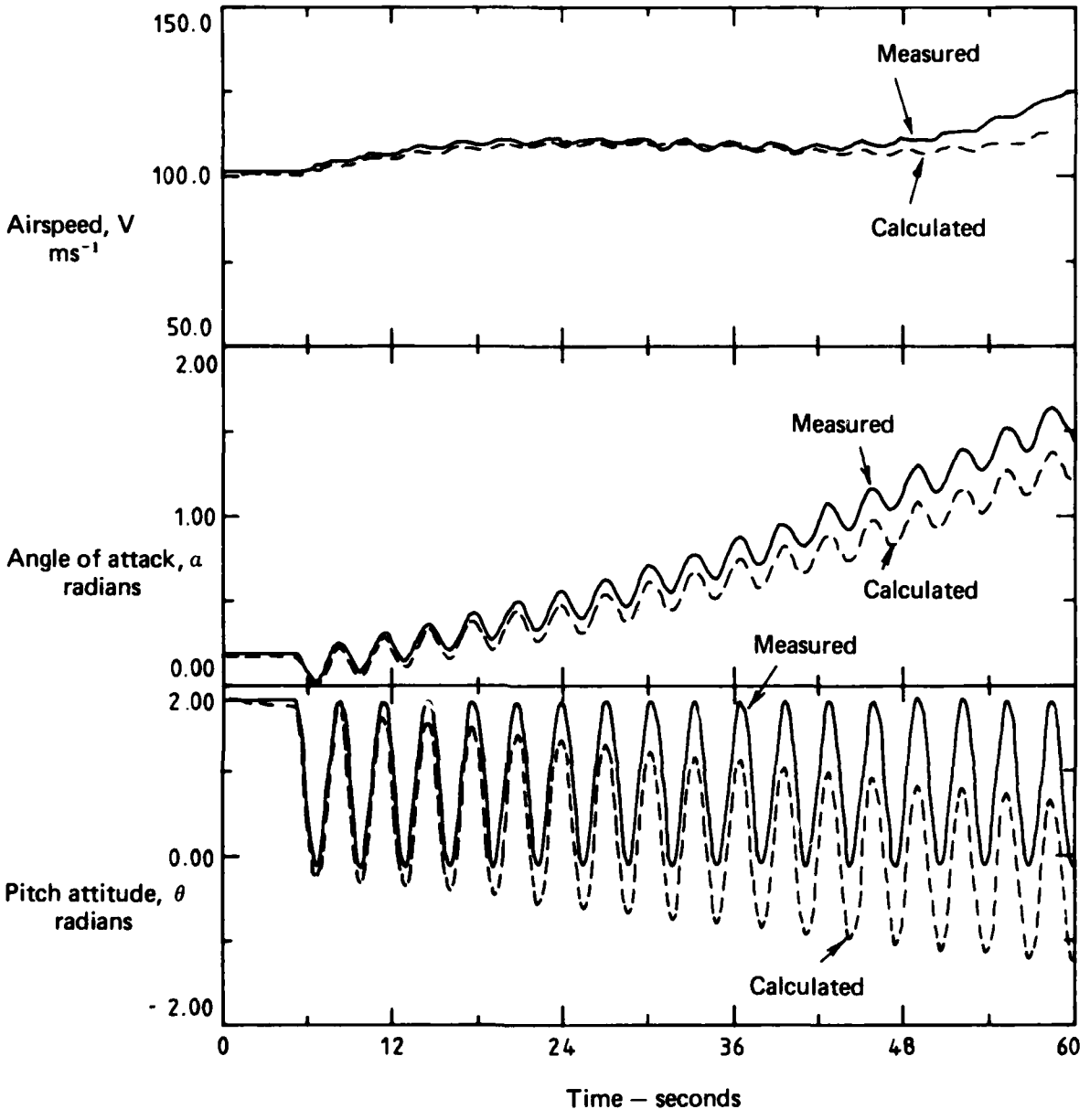

FIG. 3 MANOEUVRE 1 -- OUTPUTS

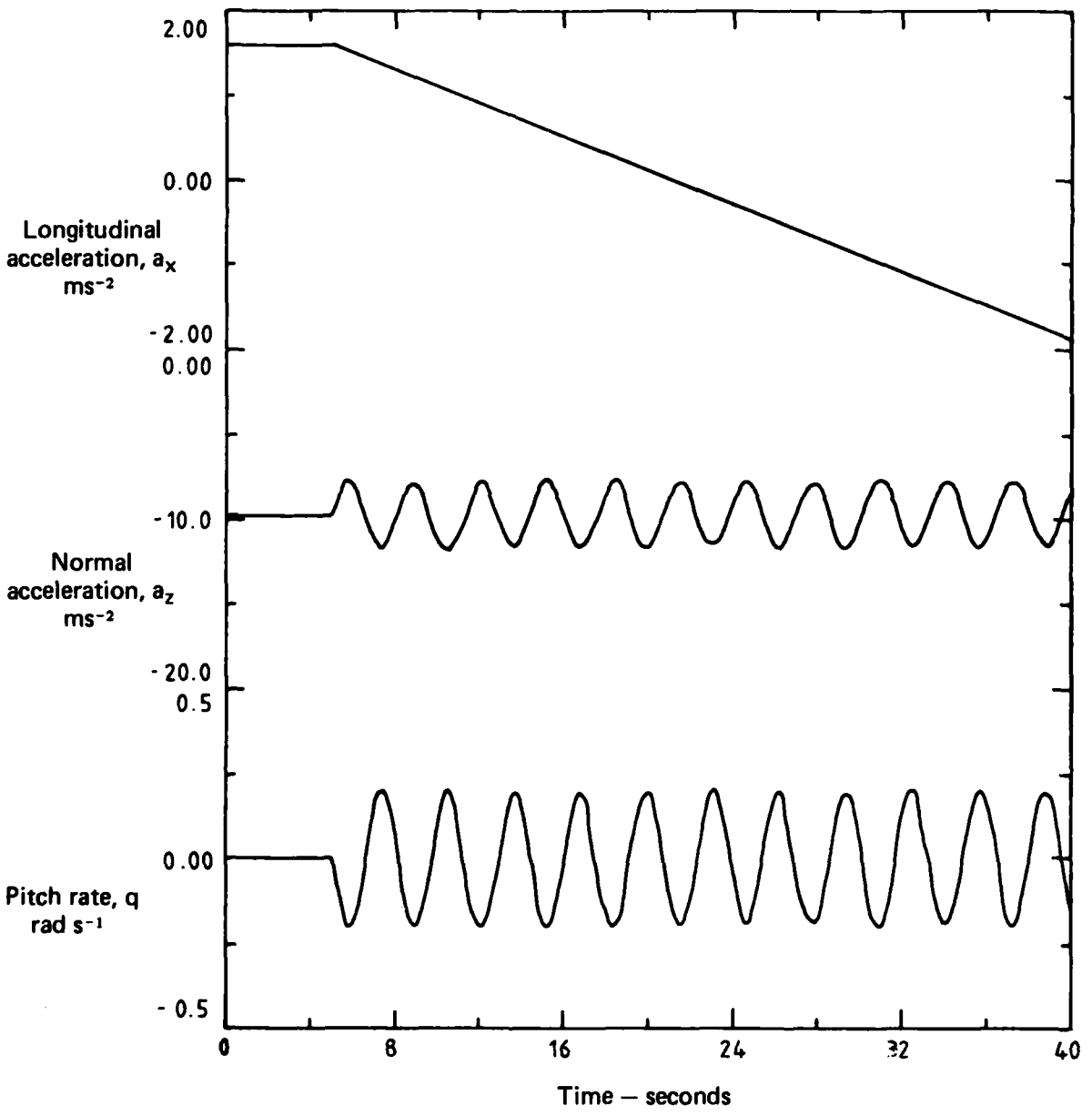

FIG. 4 MANOEUVRE 2 – INPUTS

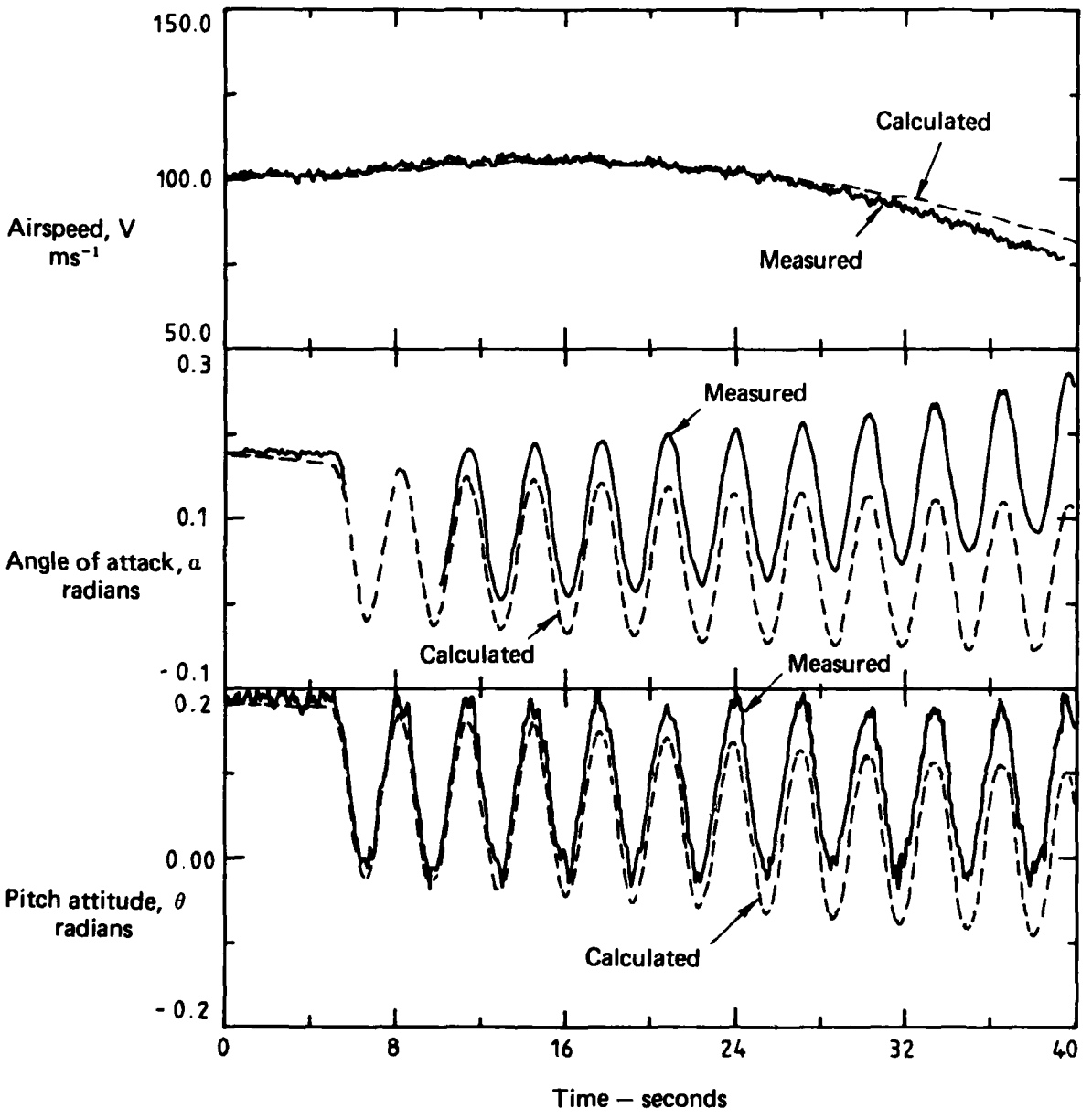

FIG. 5 MANOEUVRE 2 – OUTPUTS

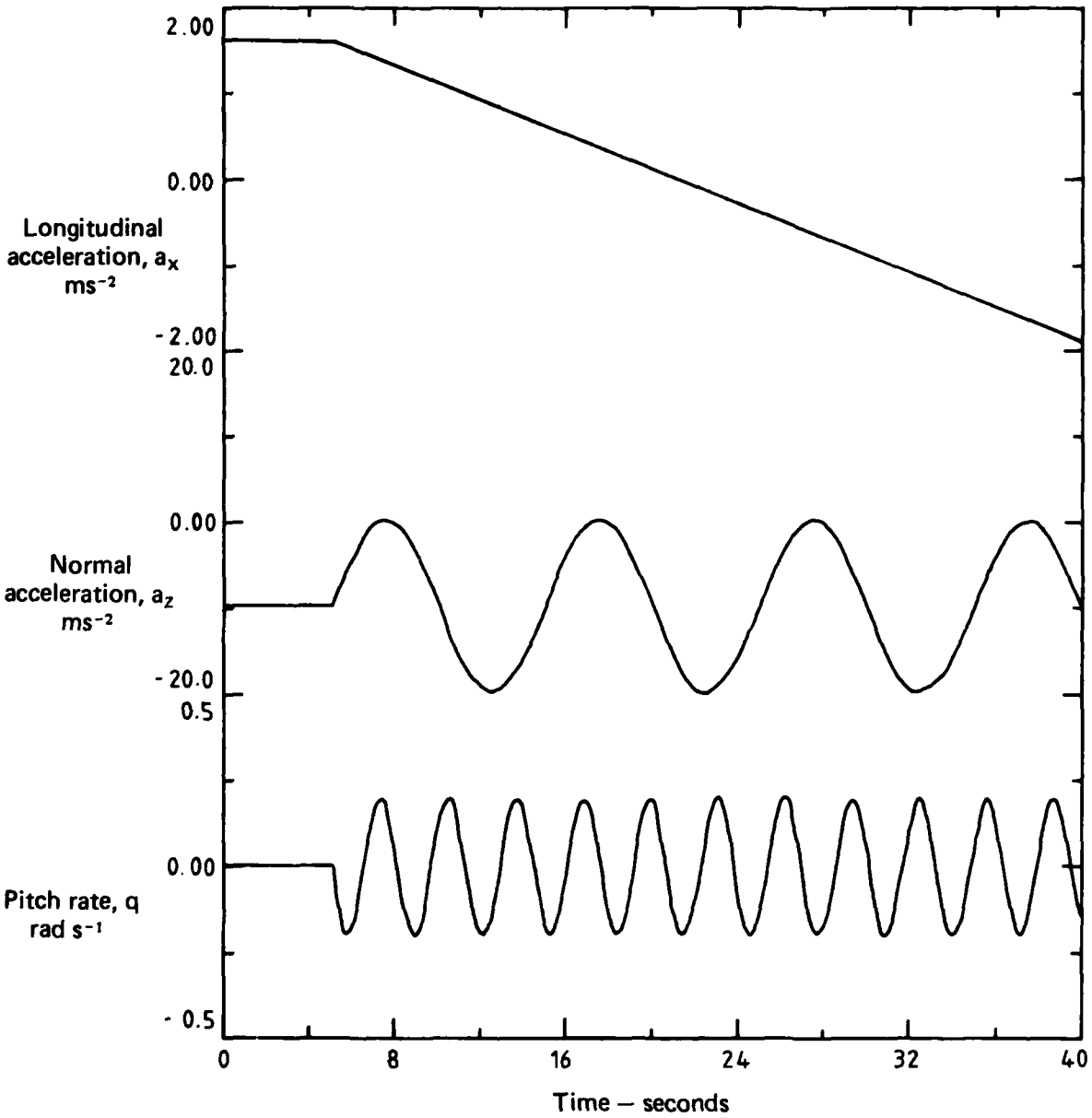

FIG. 6 MANOEUVRE 4 – INPUTS

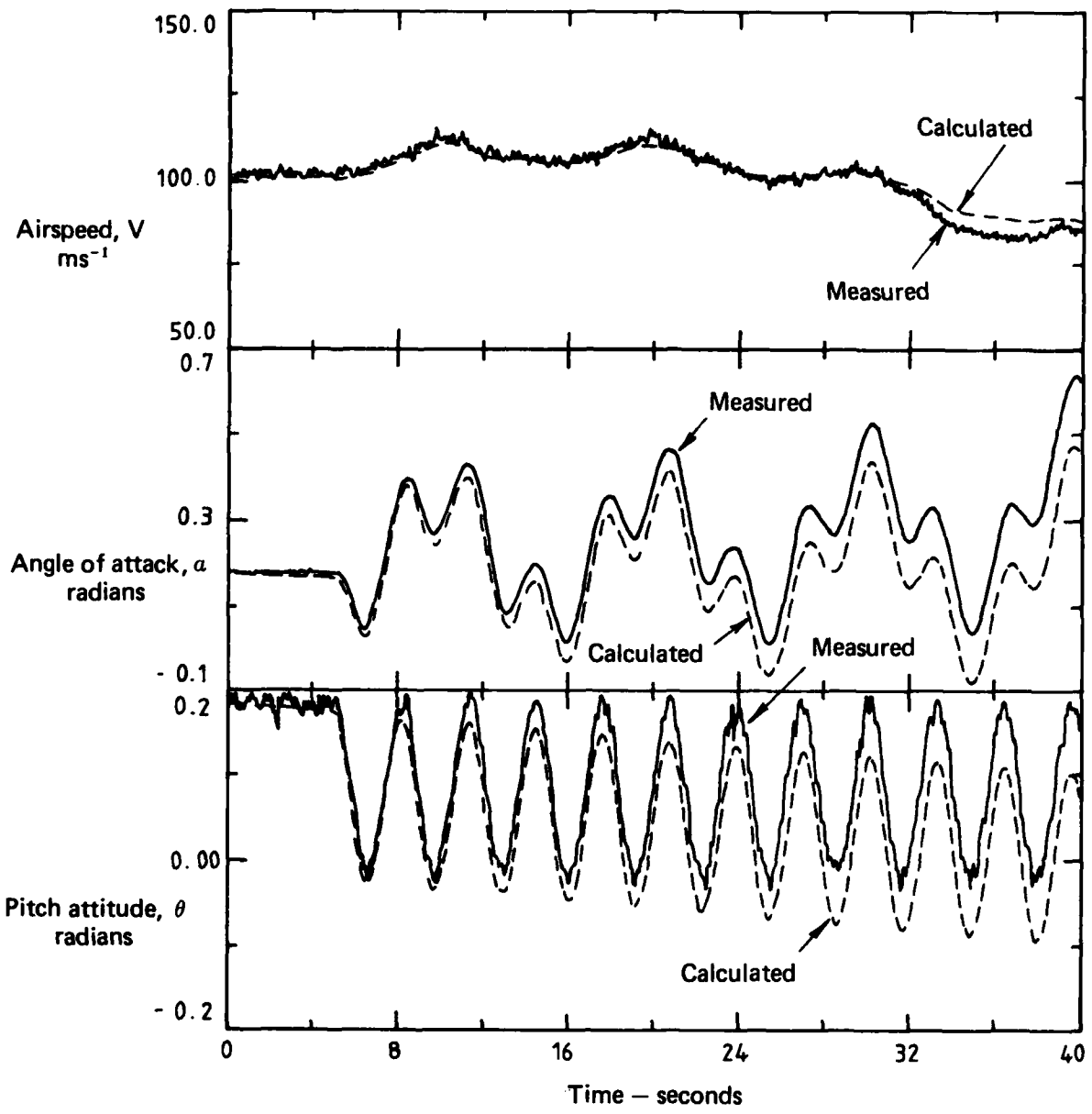

FIG. 7 MANOEUVRE 4 – OUTPUTS

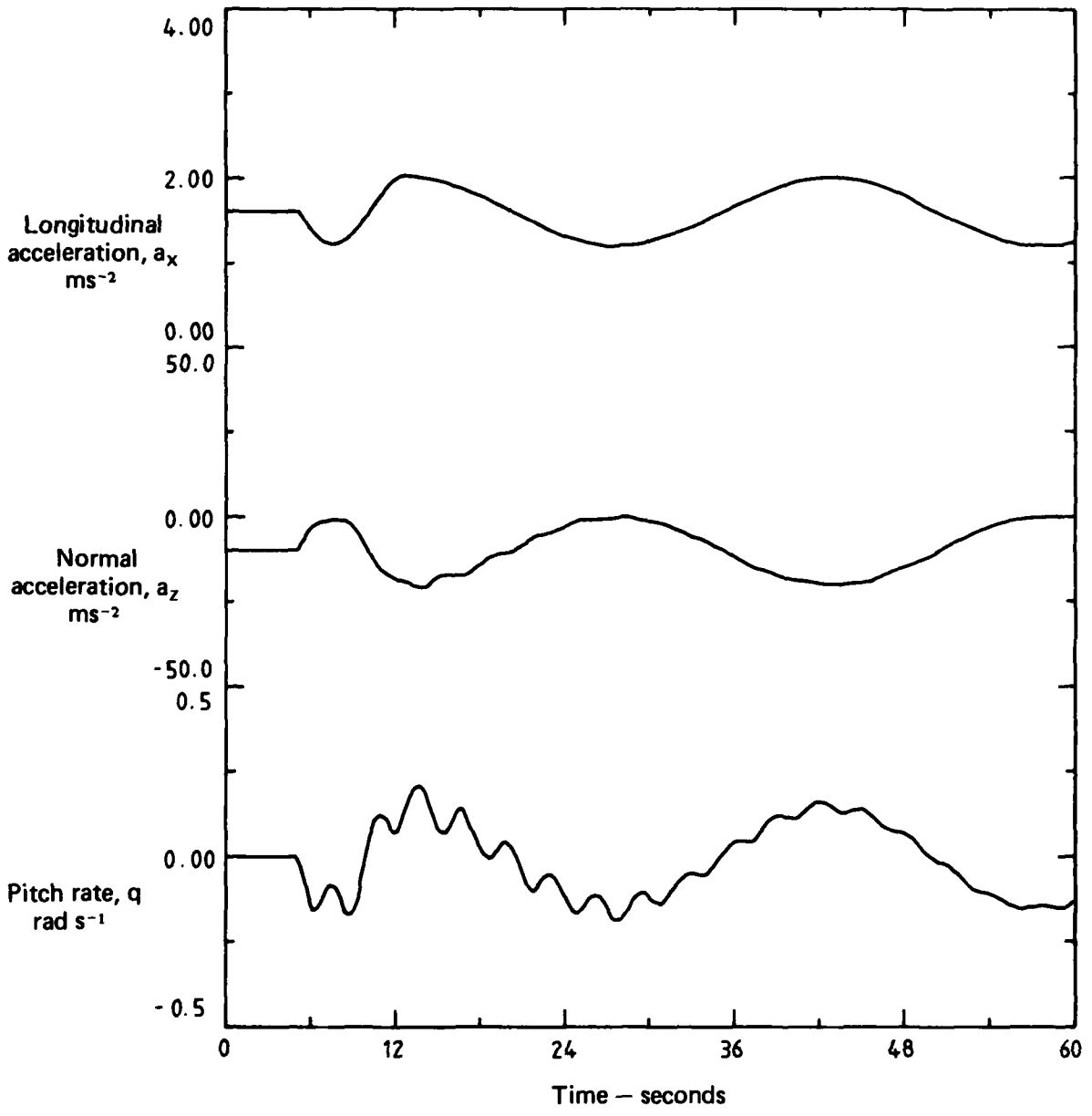

FIG. 8 MANOEUVRE 5 – INPUTS

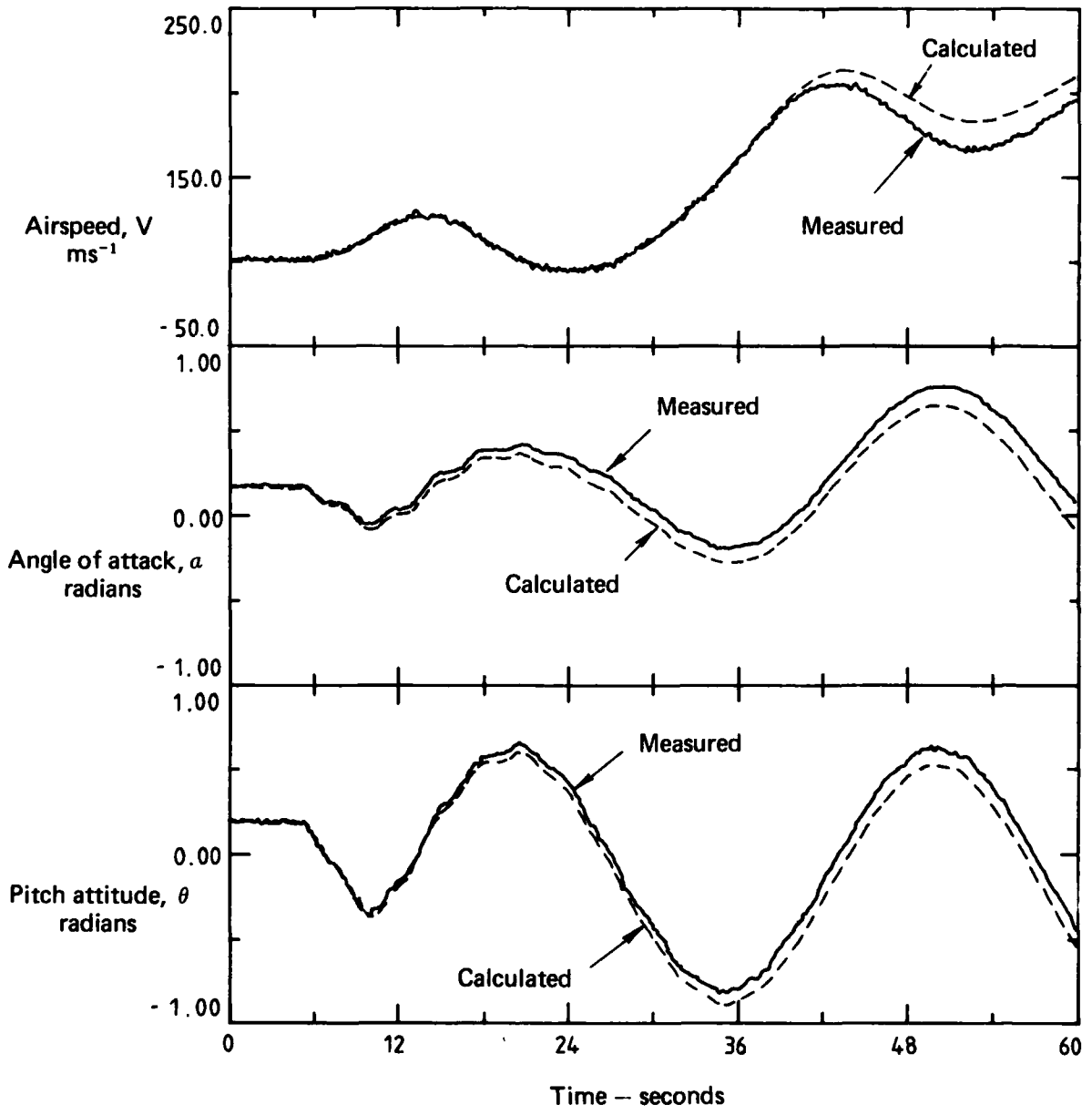

FIG. 9 MANOEUVRE 5 – OUTPUTS

DISTRIBUTION

AUSTRALIA

DEPARTMENT OF DEFENCE AND DEPARTMENT OF DEFENCE SUPPORT

Central Office

Chief Defence Scientist
Deputy Chief Defence Scientist
Superintendent, Science and Technology Programmes
Controller, Projects and Analytical Studies
} (1 copy)

Defence Science Representative (UK) (Doc. Data sheet only)
Counsellor, Defence Science (USA) (Doc. Data sheet only)
Defence Central Library
Document Exchange Centre, DISB (17 copies)
Joint Intelligence Organisation
Librarian H Block, Victoria Barracks, Melbourne
Director-General—Army Development (NSO) (4 copies)

Aeronautical Research Laboratories

Director
Library
Superintendent—Aerodynamics
Divisional File—Aerodynamics
Author: R. A. Feik
D. A. Secomb
C. A. Martin
A. J. Farrell
D. C. Collis
N. E. Gilbert
C. R. Guy
D. A. H. Bird
D. A. Frith
T. G. Ryall

Materials Research Laboratories

Director/Library

Defence Research Centre

Library
R. L. Pope

Air Force Office

Air Force Scientific Adviser
Aircraft Research and Development Unit
    Scientific Flight Group
    Library
Technical Division Library
Director-General Aircraft Engineering—Air Force
HQ Support Command (SENGSO)

Government Aircraft Factories
Manager
Library
W. Kidd

DEPARTMENT OF AVIATION
Flying Operations and Airworthiness Division

STATUTORY AND STATE AUTHORITIES AND INDUSTRY
Commonwealth Aircraft Corporation, Library
Hawker de Havilland Aust. Pty. Ltd., Bankstown, Library

UNIVERSITIES AND COLLEGES

Melbourne	Engineering Library
Newcastle	Library
	Professor G. C. Goodwin
	Dr. R. J. Evans
Sydney	Engineering Library
	Professor G. A. Bird
New South Wales	Physical Sciences Library
	Professor R. A. A. Bryant, Mechanical Engineering
RMIT	Library
	Mr. N. Mileshkin, Civil and Aeronautical Engineering

FRANCE
ONERA, Library

NETHERLANDS
National Aerospace Laboratory (NLR), Library
Delft University of Technology, J. A. Mulder

UNITED KINGDOM
Royal Aircraft Establishment
Bedford, Library
Farnborough, Library

UNITED STATES OF AMERICA
NASA Scientific and Technical Information Facility

Spares (10 copies)
Total (80 copies)

Department of Defence Support

DOCUMENT CONTROL DATA

1. a. AR No.	1. b. Establishment No.	2. Document Date	3. Task No.
AR-002-898	ARL-AERO-NOTE-411	July, 1982	DST 79/105

4. Title
A MAXIMUM LIKELIHOOD PROGRAM FOR NON-LINEAR SYSTEM IDENTIFICATION WITH APPLICATION TO AIRCRAFT FLIGHT DATA COMPATIBILITY CHECKING

5. Security
a. document: Unclassified
b. title: U. c. abstract: U.

6. No. Pages
28

7. No. Refs
15

8. Author(s)
R. A. Feik

9. Downgrading Instructions
— —

10. Corporate Author and Address
Aeronautical Research Laboratories,

P.O. Box 4331, Melbourne, Vic. 3001.

11. Authority (*as appropriate*)
a. Sponsor
b. Security
c. Downgrading
d. Approval

12. Secondary Distribution (*of this document*)
Approved for public release

Overseas enquirers outside stated limitations should be referred through ASDIS, Defence Information Services, Branch, Department of Defence, Campbell Park, CANBERRA, ACT 2601.

13. a. This document may be ANNOUNCED in catalogues and awareness services available to . . .
No limitations

13. b. Citation for other purposes (*i.e. casual announcement*) may be (select) unrestricted (or) as for 13 a.

14. Descriptors
Nonlinear systems
Flight tests
Data acquisition
Estimation
System identification
Flight path reconstruction
Maximum likelihood
Instrument errors

15. COSATI Group
0104

16. Abstract

A Fortran program has been developed for the Maximum Likelihood Estimation of parameters in non-linear systems. The program structure uses subroutines to describe the problem and define problem-specific elements, while the main program is designed to be problem-independent as far as possible. In the present note an application of the program to compatibility checking of aircraft dynamic flight test data has been studied. Using simulated time histories of longitudinal manoeuvers, the conditions for satisfactory performance have been identified. It has been shown that for a practical maneuver shape, record length and sampling rate and for reasonable noise levels on the measured data, instrument errors can be identified to good accuracy and a set of compatible time histories reconstructed.

This page is to be used to record information which is required by the Establishment for its own use but which will not be added to the DISTIS data base unless specifically requested.

16. Abstract (*Contd*)

17. Imprint

Aeronautical Research Laboratories, Melbourne

18. Document Series and Number	19. Cost Code	20. Type of Report and Period Covered
Aerodynamics Note 411	52 7730	— —

21. Computer Programs Used

COMPAT.RK4 (Fortran)

22. Establishment File Ref(s)

END

FILMED

10-83

DTIC